 doi:10.20944/preprints202208.0352.v1

A Novel Mitophagy Enhancer Protects Cardiomyocytes against Hypoxia/Reoxygenation

Xin Yan,[1#] Xiang Gao, [1#] Shanshan Hou, [1#] Steffen Jockusch,[3] K. Michael Gibson [2] * Lanrong Bi[1]*

[1] Department of Chemistry and Department of Biological Sciences, Michigan Technological University, Houghton, MI 49931, USA

[2]Department of Pharmacotherapy, College of Pharmacy and Pharmaceutical Sciences, Washington State University, Spokane WA 99202, USA

[3] Department of Chemistry, Columbia University, New York, NY 10027, USA.

* Corresponding authors: mike.gibson@wsu.edu, lanrong@mtu.edu.

Abstract: Ischemia/reperfusion (I/R) injury results in cell death by inducing apoptosis. During I/R, early generation of mitochondrial reactive oxygen species (mtROS) can induce neighboring mitochondria to release additional ROS, a toxic cycle resulting in significant mitochondrial and cellular injury. Oxidative damage in the mitochondria contributes to various pathologies, including I/R injury. Accordingly, preventing mitochondrial oxidative damage should be therapeutically relevant for many disorders, including cardiovascular diseases. We recently discovered an Indole-Peptide-Tempo Conjugate (**IPTC**) that served as a novel bifunctional agent with both antioxidant and autophagy-modulating capacity. Here, we demonstrate that **IPTC** can protect H9C2 cardiomyocytes from hypoxia/reoxygenation (H/R) injury that results from mtROS overproduction due to impaired mitophagy and resultant mitochondrial dysfunction. We hypothesize that the mechanism of action of **IPTC** involves the capacity to decrease mtROS combined with induction of mitophagy.

Keywords: Oxidative Stress, Free radical scavenging, Autophagy, Ischemia/reperfusion injury, Hypoxia/reoxygenation, Mitophagy

1. Introduction

Acute myocardial infarction (AMI) is a major source of morbidity worldwide. Prompt reperfusion strategies including pharmacological thrombolysis and percutaneous coronary intervention (PCI) have significantly improved the outlook for patients with AMI. Paradoxically, however, rapid restoration of coronary blood flow results in cardiomyocyte damage and frequent irreversible cell damage or necrosis collectively referred to as myocardial ischemia/reperfusion (M-I/R) injury [1-3]. M-I/R can further expand cardiac damage by up to 50% of the original infarct size. Clinical consequences of M-I/R include irreversible loss of contractile cardiac function and reperfusion arrhythmias. The cellular and molecular events underlying M-I/R injury are driven by multiple processes, including inflammation, endothelial dysfunction, loss of mitochondrial membrane potential, overproduction of reactive oxygen species (ROS), and platelet aggregation leading to microthrombi formation [4,5]. Overproduction of mitochondrial ROS is enhanced with the onset of reperfusion [3]. Tempol (4-hydroxy-2,2,6,6-tetramethyl-piperidine-N-oxyl) has recently garnered significant attention as an antioxidant preventing ROS accumulation. Tempol is

Preprints (www.preprints.org) | NOT PEER-REVIEWED | Posted: 18 August 2022 doi:10.20944/preprints202208.0352.v1

a stable nitroxide radical compound, and its antioxidant capacity is likely enhanced due to its superoxide dismutase (SOD)-mimicking activity [6-9].

Indole alkaloids are naturally occurring plant substances that possess a variety of neuropharmacological, psychopharmacological, and antitumor effects [10-18]. For example, the alkaloid berberine produces its anticancer effects via the induction of autophagic cell death and mitochondrial apoptosis in cancer cells [19]. Further, the indole alkaloid indole-3-carbinol represents a potent antithrombotic agent with antiplatelet activity resulting from inhibition of GP IIb/IIIa receptor and thromboxane B2 formation [20]. Additionally, indole-3-carbinol cyclic tetrameric derivative (CTet) induces autophagy and inhibits cell proliferation in both estrogen receptor-positive (MCF-7) and triple-negative (MDA-MB-231) breast cancer cell lines [21]. Here, we have sought the development of novel small molecule compounds that can prevent M-I/R injury, the latter representing a serious unmet clinical need worldwide. Our study centered on the hypothesis that conjoining an indole alkaloid scaffold, but possessing a peptide motif (RGD, arginine-glycine-aspartate) confers antiplatelet/antithrombotic capacity as seen in von Willebrand factor [22], with Tempol (i.e., Indole-Peptide-Tempo Conjugate (**IPTC**)) would result in compounds with enhanced autophagy-modulating properties that could attenuate oxidative damage and thus protect cardiomyocytes from I/R injury.

2. Materials and Methods

2.1. Synthesis of IPTC

2.1.1. Synthesis of (1S,3S)-1-methyl-2,3,4,9-tetrahydro-1H-pyrido[3,4-b]indole-3-carboxylic acid (**1**): To a solution of 0.5mL 98% H_2SO_4 in distilled water (200mL), L-Trp (5g, 25 mmol) was added in three portions. The mixture was stirred at r.t. for 15 min, and then CH_3CHO (5 mL) was added dropwise. The reaction mixture continued stirring at r.t. overnight until the precipitate appeared. Then concentrated ammonia solution (~1.5mL) was added to adjust the pH to 7.0. The formed precipitate was collected by filtration (78% yield). M.p. 287-289°C. ESI/MS 231 $[M+H]^+$. IR (KBr) 3101-2405, 2962, 2905, 1703, 1624, 1595, 1506, 1453, 1376, 1072, 904 cm^{-1}.^{1}H NMR (400 MHz, DMSO-d_6) d/ppm = 11. 92 (s, 1 H), 10. 97 (s, 1 H), 9.17 (s, 1 H), 7. 45 (d, *J* = 7. 5 Hz, 1 H), 7. 36 (t, *J* = 8.0 Hz, 1 H), 7.10 (t, *J* = 8.0 Hz, 1 H), 7.01 (t, *J* = 7.5 Hz, 1 H), 4.22 (q, *J* = 4.8Hz, 1H), 3.66 (dd, *J* = 10. 5 Hz, *J* = 5.0 Hz, 1 H), 3. 14 (dd, *J* = 10. 5Hz, *J* = 2. 4 Hz, 1 H), 2. 85 (ddd, *J* = 10. 5 Hz, *J* = 5. 0 Hz, *J* = 2. 4 Hz, 1 H), 1. 38 (d, *J* = 5.0 Hz, 3 H).

2.1.2. Synthesis of Methyl-1-methyl-1,2,3,4-tetrahydro-β-carboline-3-carboxylate (**2**): At 0 °C, to 10 ml methanol, 1 mL of thionyl chloride was added dropwise. The mixture was stirred at r.t. for 15 min, and then 2.0 g (8.7 mmol) of 1-methyl-1,2,3,4-tetrahydro-β-carboline-3-carboxylic acid **1** was added slowly. The reaction mixture was stirred at r.t. until TLC ($CHCl_3$/MeOH, 15:1) indicated the complete disappearance of 1-methyl-1,2,3,4-tetrahydro-β-carboline-3-carboxylic acid. The reaction mixture was neutralized with an aqueous solution of sodium bicarbonate (10%) to pH 7.0. The formed precipitate was collected by filtration (82% yield). ESI/MS: 245 [M+H].

Preprints (www.preprints.org) | NOT PEER-REVIEWED | Posted: 18 August 2022 doi:10.20944/preprints202208.0352.v1

2.1.3. Synthesis of Methyl-1-methyl-β-carboline-3-carboxylate (**3**): A suspension of 5.0 g (20.0 mmol) of compound **2**, 1.4 g (20. mmol) sulfur flour, and 20 ml of anhydrous dimethyl benzene was refluxed until TLC ($CHCl_3$/MeOH, 15:1) indicated the complete disappearance of compound **2**. On evaporation, the residue was dissolved in 10 mL of MeOH. After filtration and evaporation under reduced pressure, 3.2 g (65%) of compound **3** was obtained as a yellow powder. M.p. 242–243 °C; ESI/MS: 241 $[M+H]^+$; IR (KBr): 3310, 2954, 2922, 2901, 2811, 1742, 1600, 1581, 1566, 1450, 1380, 1066, 900 cm^{-1}; ^1H NMR (400MHz, DMSO-d_6): δ = 9.98 (s, 1H), 7.41 (d, J = 5.6 Hz, 1H), 7.35 (d, J = 7.2 Hz, 1H), 7.15 (d, J = 8.2 Hz, 1H), 7.11 (t, J = 7.5 Hz, 1H), 6.97 (t, J = 6.4 Hz, 1H), 3.74 (s, 3H), 2.03 (s, 3H).

2.1.4. Synthesis of 1-Methyl-β-carboline-3-carboxylic acid (**4**): To a solution of 5.0 g (20.8 mmol) of compound **(3)**, 120 ml of the aqueous solution of sodium hydroxide (2.0 mmol/L) was added and then stirred at 60 °C until TLC ($CHCl_3$/MeOH, 15:1) indicated the complete disappearance of compound **(3)**. The reaction mixture was neutralized with hydrochloric acid to pH 7.0. The formed precipitate was collected by filtration to give 3.86 g (82%) of compound **4** as a yellow powder. M.p. 292–293 °C; ESI/MS: 227 $[M+H]^+$; IR (KBr): 3230, 2252, 2924, 2910, 2900, 1700, 1610, 1585, 1562, 1440, 1380, 1066, 900 cm^{-1}; ^1H NMR ($CDCl_3$): δ = 11.06 (s, 1H), 9.88 (s, 1H), 7.42 (d, J = 5.8 Hz, 1H), 7.39 (d, J = 7.1 Hz, 1H), 7.10 (d, J = 8.0 Hz, 1H), 7.10 (t, J = 7.6 Hz, 1H), 6.99 (t, J = 6.6 Hz, 1H), 2.10 (s, 3H).

2.1.5. Synthesis of compound **6**: 0.20 mmol of hydroxybenzotriazole (HOBt) and 0.25 mmol of dicyclohexylcarbodiimide (DCC) were added to a solution containing 0.20 mmol of compound **4** in 5 mL of anhydrous THF at 0°C. The reaction mixture was stirred at 0 °C for 24 h. Precipitated dicyclohexyl urea was isolated by filtration. The filtrate was evaporated under reduced pressure, and the residue was triturated with petroleum ether to provide the corresponding ester. 0.20 mmol of tetrapeptide **(5)** and 0.26 mmol of *N*-methylmorpholine were then added to a solution of the preceding ester in 10 mL of anhydrous THF. The reaction mixture was stirred at room temperature for 24 h. Following evaporation, the residue was dissolved in 50 mL of ethyl acetate. The solution was washed with 5% sodium bicarbonate, followed by 5% citric acid and saturated sodium chloride, and the organic phase was separated and dried over anhydrous sodium sulfate. Following filtration and evaporation under reduced pressure, compound **6** was obtained by column chromatography purification ($CHCl_3$/CH_3OH, 30:1). M.p. 103 - 104 °C; $[\alpha]_D^{25}$ = - 2.38 (c = 0.375, CH_3OH + DMF); ESI/MS: 958 $[M + H]^+$; IR (KBr) 3305, 3064, 3034, 2933, 2872, 1737, 1654, 1625, 1597, 1527, 1498, 1452, 1388, 1352, 1261, 1251, 1215, 1151, 1105, 1001, 908, 785, 738, 698, 582, 516 cm^{-1}.^1H-NMR (DMSO, 400 MHz) δ /ppm= 11.96 (s, l H), 8.69 (m, 2 H), 8.52 (m, l H), 8.45 (d, J = 7.8 Hz, l H), 8.32 (d, J = 7.5 Hz, 2 H), 8.18-7.50 (m, 2 H), 7.67-7.56 (m, 2 H), 7.33-7.24 (m, 16 H), 5.16-5.10 (m, 2H), 5.06-5.01 (m, 2 H), 4.82 (q, J = 8.1 Hz, l H), 4.68 (q, J = 7.8 Hz, l H), 4.59 (q, J = 4.8 Hz, l H), 4.45 (q, J = 12 Hz, 2 H), 4.02-3.75 (m, 3 H), 3.70 - 3.63 (m, l H), 3.20 (m, 2 H), 3.02-2.83 (m, 3 H), 2. 78-2.73 (m, 2 H), 2.67-2.59 (m, l H), 1.85-1.81 (m, l H), 1.78-1.74 (m, l H), 1.57 (m, 2 H); ^{13}C-NMR (DMSO, 75 MHz) δ /ppm = 172.25, 171.05, 170.25, 170.15, 169.21, 169.11, 164.98, 159.77, 141.51, 141.34, 138.90, 138.25, 136.50, 136.46, 136.22, 136.15, 128.80, 128.63, 128.48, 128.42, 128.38, 128.34, 128.27, 128.13, 127.95, 127.91, 127.06, 126.88, 122.53, 121.91, 120.45, 112.76, 112.71, 72.74, 69.48, 66.59, 66.15, 53.15, 52.46, 49.53, 42.40, 36.81, 30.83, 25.25, 20.91.

Preprints (www.preprints.org) | NOT PEER-REVIEWED | Posted: 18 August 2022 doi:10.20944/preprints202208.0352.v1

2.1.6. Synthesis of compound **7**: 0.2 mmol of compound **6** was added to 1 mL of phenyl methyl ether, 1 mL of dimethyl sulfide, and 4 mL of HF and stirred at 0 °C for 2 h. The reaction mixture was evaporated under reduced pressure and the residue was then triturated with petroleum ether. The triturated residue was further purified on Sephadex G-10 followed by HPLC purification (56% yield). M.p. 78-79°C. $[\alpha]_D^{25}$ = -6.64 (c = 0.5, H_2O). ESI/MS: 642 $[M+H]^+$; IR (KBr) 3278, 3199, 2785, 2318, 1668, 1533, 1465, 1400, 1278, 1255, 1170, 1114, 1031, 896, 866, 667, 640, 576, 518, 457 cm^{-1}; ^{1}H-NMR (DMSO, 400 MHz) δ /ppm= 12.03 (s, l H), 8.70 (m, 2 H), 8.34 (d, *J* = 7.8 Hz, l H), 7.74 (m, l H), 7.66 - 7.56 (m, 3 H), 7.31-7.26 (m, 4 H), 4.65 (m, l H), 4.58 (m, 2 H), 4.15 (m, 2 H), 3.88-3.58 (m, 4 H), 3.15-3.07 (m, 2 H), 2.85 (m, 3 H), 2.71 (m, l H), 2.58 (m, l H), 2.45 (m, 3 H), 1.94 (m, l H), 1.77 (m, l H), 1.56 (m, 2 H). ^{13}C-NMR (DMSO, 75 MHz) δ /ppm = 172.80, 172.46, 171.07, 169.03, 164.93, 157.31, 141.55, 141.34, 138.83, 136.50, 128.83, 127.88, 123.30, 122.57, 121.87, 120.46, 119.03, 112.74, 65.14, 61.89, 54.21, 49.86, 44.67, 42.52, 36.99, 30.86, 25. 30, 20.95.

2.1.7. Synthesis of ***IPTC****:* At 0°C, 4-amino Tempo (1.6mmol), and a catalytic amount of HOBt were added to a solution of compound **7** (1.5mmol) in CH_2Cl_2, 1-ethyl-3-(3-dimethylaminopropyl) carbodiimide (EDC) (1.6mmol). The pH was adjusted to 8-9. The reaction mixture was stirred under argon until TLC analysis indicated the complete disappearance of compound **7**. The solvent was evaporated under vacuum and the crude residue was further purified by flash chromatography to give the target compound, **IPTC**, as an orange powder (45% yield). HRMS(ESI) m/z for $C_{37}H_{52}N_{11}O_9$: 794.3949; found: 794.3963.

2.2. PC12 cell survival assay: [23-30] The free radical scavenging capacity of the newly synthesized compound IPTC was evaluated in PC12 cells using the method of Dawson with minor modifications. In brief, PC12 cells were grown in Dulbecco's modified Eagle's medium supplemented with 10% heat-inactivated horse serum (Hyclone), 5% fetal bovine serum (GIBCO), 1.0 mM sodium pyruvate, 100 U/mL penicillin, and 100 µg/mL streptomycin at 37 °C, in 5% CO_2 atmosphere. PC12 cells were seeded in 96-well plates coated with poly-L-lysine at a density of 20,000 cells per well during the exponential phase of growth. After a 24 h attachment period fresh media containing 12.5, 25, 50, 100, or 200 µM of **IPTC**, respectively, were added to each well and were incubated for 1 h. Nitric oxide (NO) damage was then induced by adding 2 mM of sodium nitroprusside (SNP) followed by 2 h of incubation [31]. The media were replaced with fresh media and cells were incubated for 14 h, after which cell survival was measured by a colorimetric assay with MTT according to the method of Mosmann [32]. Similarly, H_2O_2 damage was induced with 1 mM H_2O_2 followed by 1 h of incubation, while hydroxy-radical (•OH) damage was induced by 1 mM H_2O_2/30 µM Fe (II) followed by 1 h of incubation [32]. Statistical analysis employed a one-way ANOVA test.

2.3. Hypoxia/reoxygenation (H/R) protocol: H9C2 cardiomyocytes have been routinely used as a cellular model of cardiac ischemia/reperfusion (I/R) injury in vitro [39]. Rat cardiomyocytes H9C2 were cultured in Dulbecco's Modified Eagle's Medium/Nutrient Mixture F-12 (DMEM/F12) supplemented with 10% (v/v) fetal bovine serum (FBS, Invitrogen Life Technologies), 100 µg/mL of penicillin and 100 µg/mL of streptomycin. Cells were cultured to 70%-80% confluence for further experiments. We examined the putative pro-

Preprints (www.preprints.org) | NOT PEER-REVIEWED | Posted: 18 August 2022 doi:10.20944/preprints202208.0352.v1

tective effects of **IPTC** in rat cardiomyocytes H9C2 using the cellular model of hypoxia/reoxygenation (H/R), which was achieved in a flow-through chamber as previously described [39]. In brief, H9C2 cells were subjected to hypoxia using glucose-free and FBS-free DMEM/F12 buffer in a flow-through chamber supplied with 94% N_2, 5% CO_2, and 1% O_2 at 37°C for 6 h. After hypoxia, the cells were transferred back to 10% FBS and DMEM/F12 under normal conditions for reoxygenation for 4 h. Normal control cells were incubated in a regular cell culture incubator under normoxic conditions.

H9C2 cells were divided into 12 groups: (1) Sham-control group, cells were cultured under normal conditions; (2) Control + Tempol group, cells were cultured with Tempol (10 μM) under normal conditions; (3) Control + Mito-Tempo groups, cells were cultured with Mito-Tempo (10 μM) under normal conditions. Mito-Tempo is a mitochondria-targeted antioxidant. The chemical structure of Mito-Tempo contains a piperidine nitroxide (Tempo) with the lipophilic cation triphenylphosphonium (TPP^+) [40]. (4) Control + **IPTC** groups, cells were cultured with **IPTC** (10 μM) under normal conditions. (5) Hypoxia (H) group, cells were subjected to 6h of hypoxia (H) protocol; (6) Hypoxia + Tempol (10 μM) group, cells pretreated with Tempol for 12 h before induction of hypoxia and then subjected to 6h of hypoxia; (7) Hypoxia + Mito-Tempo (10 μM) group, cells pretreated with Mito-Tempo for 12 h before induction of hypoxia and then subjected to 6h of hypoxia; (8) Hypoxia + **IPTC** (10 μM) group, cells pretreated with **IPTC** for 12 h before induction of hypoxia and then subjected to 6h of hypoxia; (9) H/R group, cells were subjected to hypoxia/reoxygenation protocol (H/R); (10) H/R + Tempol (10 μM) group, cells pretreated with Tempol for 12 h before induction of hypoxia and then subjected to H/R protocol; (11) H/R + Mito-Tempo (10 μM) group, cells pretreated with Mito-Tempo for 12 h before induction of hypoxia and then subjected to H/R protocol; (12) H/R + **IPTC** (10 μM) group, cells pretreated with **IPTC** for 12 h before induction of hypoxia and then subjected to H/R protocol.

Cell viability assay: Cell viability was evaluated with the CCK-8 kit by a microplate reader at a wavelength of 450 nm. Cell counting kit-8 (CCK-8) is a colorimetric assay for the determination of the number of viable cells in the cytotoxicity assay, which is more sensitive than any other tetrazolium salts such as MTT. Each experiment was repeated 3 times, and the results are shown in **Figure 1**. Data are expressed as a percentage of the sham control and are represented as mean ± SD (n = 6; #: $p < 0.05$; *: $p < 0.01$ *vs* H/R alone group).

Detection of lactate dehydrogenase (LDH): The LDH release assay is a cell cytotoxicity assay used for the assessment of plasma membrane damage in a cellular population. In this assay, LDH reduces NAD to NADH, which then interacts with a specific probe to produce a color (OD max = 450nm). The levels of LDH in cell supernatants were detected using commercially available kits by following the manufacturer's protocol. In brief, the cell supernatants were collected and then incubated with the reagents of the LDH assay kit. LDH activity was quantified by a microplate reader at OD450nm. LDH activity was expressed as (U/L), and the results are shown in **Figure 2**. The irreversible injury was quantitated as the percent total LDH released (values are expressed as mean ± SD; n = 6).

Detection of Mitochondrial ROS generation: Cardiomyocytes H9C2 were counter-

 doi:10.20944/preprints202208.0352.v1

stained with MitoProbe and Hoechst 33342, respectively. MitoProbe is a group of novel fluorogenic probes specifically localized in mitochondria and can be employed both *in vivo* and *in vitro* for the detection of mitochondrial ROS generation [33-39]. Mitochondrial ROS (mtROS) generation and the mitochondrial morphology changes can be directly visualized under confocal fluorescence microscopy (**Figure 3A**) using cell samples subjected to the same H/R protocol. The generation of mtROS and the alterations of mitochondrial morphology were simultaneously examined at three different time points of H/R (i) 0 h (before cells were subjected to H/R; (ii) immediately after 6h of hypoxia; (iii) immediately after 6h of hypoxia followed by 4h of reoxygenation. Before quantifying the alterations of the mean fluorescence intensity (MFI) of MitoProbe, the confocal fluorescence images were pre-processed (**Figure 3B**) to improve the quality of binarized images. By measuring the MFI of MitoProbe changes in the binarized images, the total ROS generation in the mitochondria was quantitatively determined and the results are shown in **Figure 3C**. Error bars indicate the standard error of the mean (SEM) from at least four independent experiments. (#: compared with control at baseline, $p < 0.01$; ∗: compared with H/R alone, $p < 0.01$).

Mitochondrial morphology analysis: Cells were counter-stained with MitoTracker (green fluorescence) for mitochondrial morphological analysis. The mitochondrial morphology was classified into three categories: tubular (normal), intermediate (tubular with swollen regions), and fragmented (small and globular) (**Figure 3D**). The method for quantification involved determining the percentage of cells with abnormal mitochondrial morphologies as a surrogate for the proportion of cells with fragmented mitochondria. When cells with intermediate or fragmented mitochondria were expressed as a percentage of the total cells counted (100 cells were counted per experiment and the data was averaged over four independent experiments per treatment), the non-treated cells contained predominantly long and evenly distributed tubular mitochondria throughout the cell. Error bars indicate SEM from at least four independent experiments (#: compared with H/R alone, $p < 0.05$; *: compared with H/R alone, $p < 0.01$). The results were presented in **Figure 3E**.

Detection of malondialdehyde (MDA): Protein concentrations of lysis buffer were measured by enhanced bicinchoninic acid (BCA) protein assay kit. MDA is a commonly used marker for oxidative stress. For detection of MDA, the cell lysis buffers were incubated with the reagents of the MDA assay kit, and this kit allows the quantitation of MDA-protein adduct. MDA level was expressed as nmol/ (mg protein), and the results are shown in **Figure 4**. Values are expressed as mean ± SD; n = 3.

Detection of mitophagy: Microscopy-based green fluorescent protein GFP-LC3 puncta formation assay is a commonly used assay for measuring autophagic activity [71]. To further examine the effect of **IPTC** on the degradation of mitochondria by autophagy (mitophagy), H9C2 cells were transfected with GFP-LC3. Then GFP-LC3 transfected H9C2 cells were co-stained with MitoProbe. Rapamycin is a known inducer of autophagy [41]. Herein, rapamycin was used as a positive control in our present study. 10 fields of view were randomly selected for each sample, and the percentages of cells with GFP-LC3 positive punctate, MitoProbe positive, and their colocalization (dual-positive, GFP-LC3+/MitoProbe+) were calculated, respectively, and the results are shown in **Figure 5**.

Preprints (www.preprints.org) | NOT PEER-REVIEWED | Posted: 18 August 2022 doi:10.20944/preprints202208.0352.v1

In this assay, H9C2 cells were divided into five groups: (1) Sham-control group, cells were cultured under normal conditions; (2) Hypoxia (H) group, cells were subjected to 6h of hypoxia (H); (3) H/R group, cells were subjected to hypoxia/reoxygenation protocol (H/R); (4) H/R + rapamycin (10 μM) group, cells pretreated with rapamycin for 12 h before induction of hypoxia and then subjected to H/R protocol; (5) H/R + **IPTC** (10 μM) group, cells pretreated with **IPTC** for 12 h before induction of hypoxia and then subjected to H/R protocol.

Detection of mitochondrial permeability transition pore (mPTP) opening: In this assay, H9C2 cells were divided into nine groups: (1) Sham-control group; (2) Control + rapamycin (10 μM) group; cells were cultured with rapamycin (10 μM) under normal conditions. (3) Control + **IPTC** (10 μM) groups; cells were cultured with **IPTC** (10 μM) under normal conditions. (4) Hypoxia (H) group, cells were subjected to 6h of hypoxia (H); (5) Hypoxia + rapamycin (10 μM) group, cells pretreated with rapamycin for 12 h before induction of hypoxia and then subjected to 6h of hypoxia; (6) Hypoxia + **IPTC** (10 μM) group, cells pretreated with **IPTC** for 12 h before induction of hypoxia and then subjected to 6h of hypoxia; (7) H/R group, cells were subjected to hypoxia/reoxygenation protocol (H/R); (8) H/R + rapamycin (10 μM) group, cells pretreated with rapamycin for 12 h before induction of hypoxia and then subjected to H/R protocol; (9) H/R + **IPTC** (10 μM) group, cells pretreated with **IPTC** for 12 h before induction of hypoxia and then subjected to H/R protocol.

Briefly, rat cardiomyocytes H9C2 were incubated with calcein (fluorescein complex; 2 μM) and $CoCl_2$ (1 mM) in Hank's Balanced Salt Solution (HBSS)/Ca^{2+} at 37°C for 15 min. Calcein can passively diffuse into cells. Calcein-AM is a membrane-permeable fluorophore. It can easily diffuse into all subcellular compartments including mitochondria [42]. The acetoxymethyl (AM) group of the fluorophore can be readily cleaved by ubiquitous intracellular esterase. Because of its hydrophilicity, calcein is then trapped within all subcellular compartments. Thus, calcein can accumulate in the cytosol and mitochondria and its corresponding fluorescence can be observed. The cells are then loaded with the divalent cobalt cation (Co^{2+}). $CoCl_2$ can quench the cytosolic fluorescence, whereas the fluorescence from the mitochondria can be maintained because of the intact inner mitochondrial membrane [42]. The opening of the mitochondrial permeability transition pore (mPTP) enables cobalt to enter mitochondria thereby resulting in the quenching of calcein fluorescence in the mitochondria. Before quantifying the alterations of the mean fluorescence intensity (MFI) of the calcein fluorescence, the confocal fluorescence images were pre-processed to improve the quality of binarized images. Error bars indicate the standard error of the mean (SEM) from at least four independent experiments. The results are shown in **Figure 6**.

3. Results

*3.1. Synthesis of **IPTC***: Starting from the optically active L-tryptophan, following esterification of the carboxylic moiety with MeOH/$SOCl_2$, the resulting L-tryptophan methyl ester was then subjected to Pictet–Spengler cyclization with acetaldehyde to yield 1-methyl-1,2,3,4-tetrahydro-β-carboline-3-carboxylate **2** in 45% yield. The conversion of the 1,2,3,4-tetrahydro-β-carboline derivative **2** to the corresponding β-carboline derivative **3** (67% yield) was carried out via oxidation of the tetrahydro-β-carboline derivatives

Preprints (www.preprints.org) | NOT PEER-REVIEWED | Posted: 18 August 2022 doi:10.20944/preprints202208.0352.v1

with sulfur in refluxing xylene. Subsequently, compound **3** was hydrolyzed in the presence of sodium hydroxide to provide the key intermediate **4** (83% yield). The protected tetrapeptide intermediates were prepared according to the synthetic route shown in **Scheme 1**. The protected tetrapeptide intermediate **5** was prepared via the solution method. The conjugation of **4** and the protected tetrapeptide fragment **5** subsequently proceeded smoothly to give compound **6**. After removal of the protecting groups, compound **7** was subjected to conjugation with 4-amino Tempo, and the desired product **IPTC** was obtained in moderate yield (45% yield).

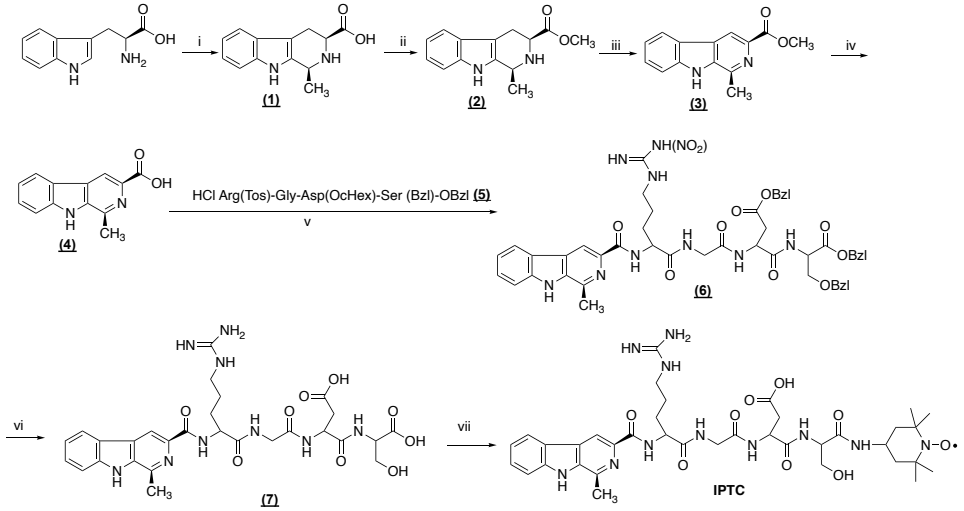

Scheme 1: Synthetic route for **IPTC**. Reagents: (i) H_2SO_4, CH_3CHO; (ii) $SOCl_2$; (iii) Sulfur; (iv) NaOH(aq); (v) compound **5**, N,N′-dicyclohexylcarbodiimide (DCC); (vi) hydrogen fluoride (HF); (vii) 4-amino-Tempo, DCC.

*3.2. In vitro antioxidant and free radical scavenging activity of **IPTC** evaluated in PC 12 cell lines:* Rat pheochromocytoma (PC12) cells that originate from the adrenal medulla, synthesize and release catecholamines. PC12 cells are very sensitive to oxidative stress, and it has been extensively used for *in vitro* ischemia studies [23-30]. Herein, the free radical scavenging properties of **IPTC** against •NO, •OH, and H_2O_2 were evaluated using PC12 cell survival assay and compared with that of Tempol. The results were expressed as EC_{50} (μM) values. The reduction of viability induced by exposure to free radicals was curtailed with incubation of **IPTC** or Tempol. We found that **IPTC** exhibited significantly better hydroxyl radical scavenging than Tempol ($p < 0.001$) or its precursor compound **4** ($p < 0.001$). In addition, we observed that **IPTC** showed a clear better protecting ability against H_2O_2 than Tempol ($p < 0.01$) or its precursor compound **4** ($p < 0.01$). Furthermore, we found that **IPTC** exhibited comparable or better protection against •NO than its precursor, compound **4**, or Tempol (**Table 1**).

Table 1. Free radical scavenging activity of **IPTC** tested in PC12 cell survival assays

Compound	EC_{50} (μM) (X ± SD)		
	EC_{50}/•NO	EC_{50}/H_2O_2	EC_{50}/•OH
Tempol	90.4 ± 4.5	65.7 ± 2.8	84.3 ± 3.2
Compound **4**	88.7 ± 4.6	56.4 ± 4.3	91.0 ± 4.7
IPTC	61.5 ± 3.7	31.3 ± 3.4##	15.7 ± 2.5***

##: $p < 0.01$; ***: $p < 0.001$.

Preprints (www.preprints.org) | NOT PEER-REVIEWED | Posted: 18 August 2022 doi:10.20944/preprints202208.0352.v1

3.3. IPTC improved cell viability of H9C2 cells subjected to hypoxia/reoxygenation (H/R) protocol:

The vulnerability of H9C2 cardiomyocytes to hypoxia and H/R-induced oxidative stress was determined by cell viability. Cell viability was tested by CCK-8 assay. Analysis of cell viability demonstrated that H9C2 cells are sensitive to H/R injury. Compared to the control group, the cell viability of the H/R groups was significantly reduced ($p < 0.01$). The effects of drug (Tempol, Mito-Tempo, and **IPTC**) pretreatment on the cell viability of H9C2 subjected to H/R were presented in **Figure 1**. The pretreatment with Tempo, Mito-Tempo, or **IPTC** could prevent the loss of H9C2 cells to a different extent. There is a significant difference between Mito-Tempo + H/R groups compared to the H/R group alone ($p < 0.01$). When compared to Mito-Tempo, **IPTC** exhibited slightly better cytoprotective activities, but there is no statistical difference.

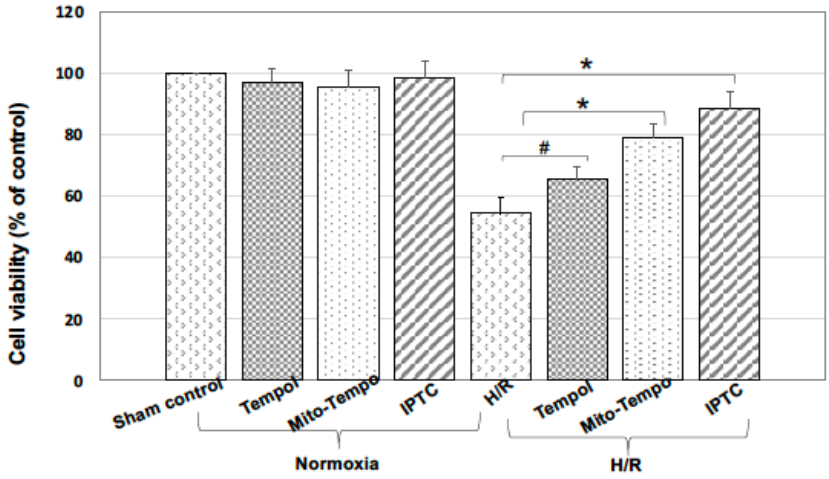

Figure 1. Effect of the tested compounds (Tempol, Mito-Tempo, and **IPTC**) on the cell viability of H9C2 cells subjected to H/R protocol.

3.4. ***IPTC*** *reduced LDH level in H9C2 cells subjected to H/R*: The LDH (lactate dehydrogenase) release assay is a routinely used assay for the assessment of cytotoxicity assay by monitoring the level of plasma membrane damage in the cell population. As shown in **Figure 2**., the basal LDH release of cells from sham-control groups was 8.9 ± 2.1%. Under normoxic conditions, there was no noticeable effect observed on basal LDH release after pre-incubation with Tempol/Mito-Tempol/**IPTC** alone. During H/R, a substantial number of cells were irreversibly injured, as shown by the release of 66.5 ± 4.2% of total cellular LDH. The pretreatment with Tempol/Mito-Tempo/**IPTC** had similar protective effects against lethal cell injury, and they reduced hypoxic injury to a different extent. Of note, pretreatment with **IPTC** followed by H/R protocol could dramatically limit lethal cell injury (28.8 ± 3.4%). Compared to the sham control group, the expression of LDH was higher in the H/R group ($p < 0.01$). During H/R, Mito-Tempol ($p < 0.01$) or **IPTC** pretreatment ($p < 0.01$) remarkably reduced the level of LDH. No significant difference was observed between **IPTC-** and Mito-Tempo pretreatment groups.

Preprints (www.preprints.org) | NOT PEER-REVIEWED | Posted: 18 August 2022 doi:10.20944/preprints202208.0352.v1

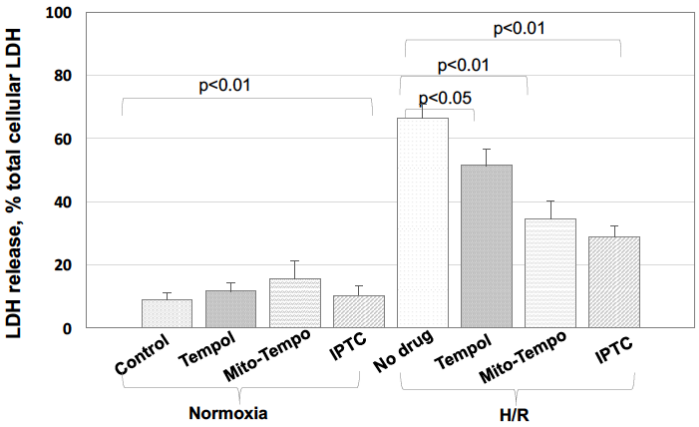

Figure 2. Effect of the tested compounds (Tempol, Mito-Tempo, and IPTC) on the lethal injury of H9C2 cells induced by H/R. Cells were exposed to the tested compounds for 12h prior to being subjected to hypoxia for 6h and reoxygenation for 4h.

*3.5. **IPTC** inhibited mitochondrial fragmentation and mitochondria-derived ROS (mtROS) production in H9C2 cells subjected to H/R protocol:*

During hypoxia, selected cells displayed enhanced MitoProbe signals with fluorescence restricted to the tubular network surrounding the nucleus (row 2, **Figure 3A**). Conversely, reoxygenation resulted in dispersed and irregular staining in cells with enhanced fluorescence. Increases in MitoProbe fluorescence relative to baseline values were evident during H/R. Pretreatment with either Mito-Tempo or **IPTC** significantly attenuated the increase in MitoProbe fluorescence intensity during H/R. By measuring the fluorescence intensity of MitoProbe changes at different time points of H/R, the total ROS generation in the mitochondria was quantified. In our current studies, we observed a ~2.5-fold increase of mtROS during the hypoxia phase (row 2, **Figure 3A;** see **Figure 3C** for quantitative values), while 6h of hypoxia followed by 4h of reoxygenation resulted in a ~7.4-fold elevation of mtROS (row 3, **Figure 3A;** see **Figure 3C** for quantitative values). Cells pretreated with either Mito-Tempo or **IPTC** manifested much lower mtROS levels, suggesting that elevated mtROS generation induced by H/R could be significantly mitigated by Mito-Tempo (row 5, **Figure 3A;** see **Figure 3C** for quantitative values) or **IPTC** intervention (row 6, **Figure 3A;** see **Figure 3C** for quantitative values).

Next, we addressed the effect of **IPTC** on mitochondrial morphology. Mitochondria in sham control cells are long tubular structures (illustration image see row 1, **Figure 3D**) with weak fluorescence of MitoProbe. The number of cells with intermediate (illustration image see row 2, **Figure 3D**) and fragmented mitochondria increased significantly during hypoxia and was found to significantly increase the percentage of cells with intermediate or fragmented mitochondria when compared to control cells, whereas reoxygenation resulted in most cells displaying fragmented mitochondria with shorter and spherical structures (illustration image see row 3, **Figure 3D**). The percent of cells exhibiting long tubular mitochondria decreased from 81.3 ± 5.4% (sham control) to 9.8 ± 2.3% (H/R alone), while mitochondria with intermediate and fragmented morphology were predominantly aggregated in the perinuclear region (row 3, **Figure 3A**). Mito-Tempo or **IPTC** addition to the control cell perfusate undergoing hypoxia resulted in significant protection against H/R induced cell death and attenuated the fragmented mitochondrial appearance. The cells treated with **IPTC** + H/R significantly decreased the percentage of cells with fragmented mitochondria (**IPTC** + H/R: 85.7 ± 4.5% *vs*. H/R alone: 11.5 ± 2.6%) (row 6, **Figure 3A**; see **Figure 3E** for quantitative values).

Preprints (www.preprints.org) | NOT PEER-REVIEWED | Posted: 18 August 2022 doi:10.20944/preprints202208.0352.v1

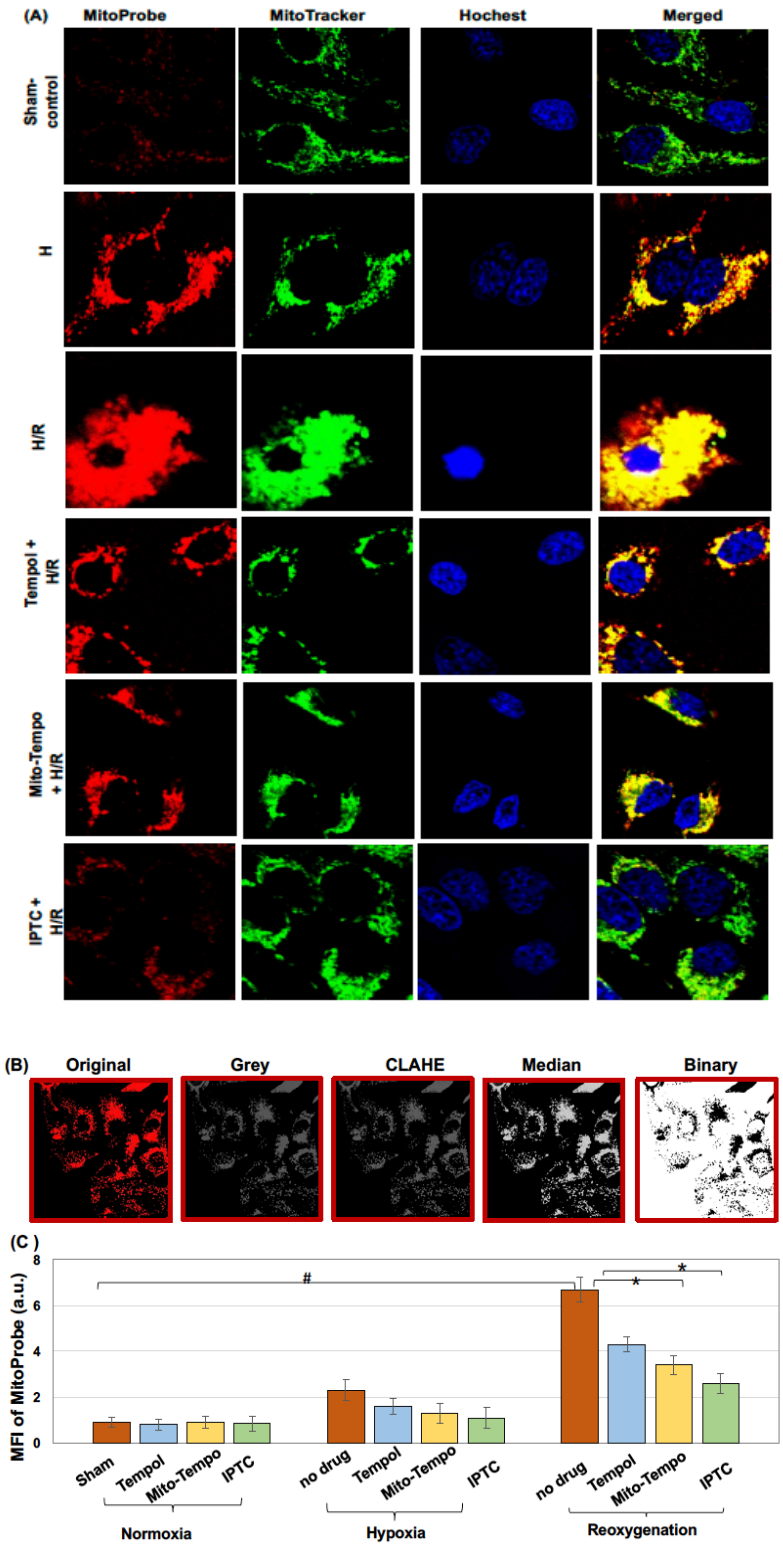

Preprints (www.preprints.org) | NOT PEER-REVIEWED | Posted: 18 August 2022 doi:10.20944/preprints202208.0352.v1

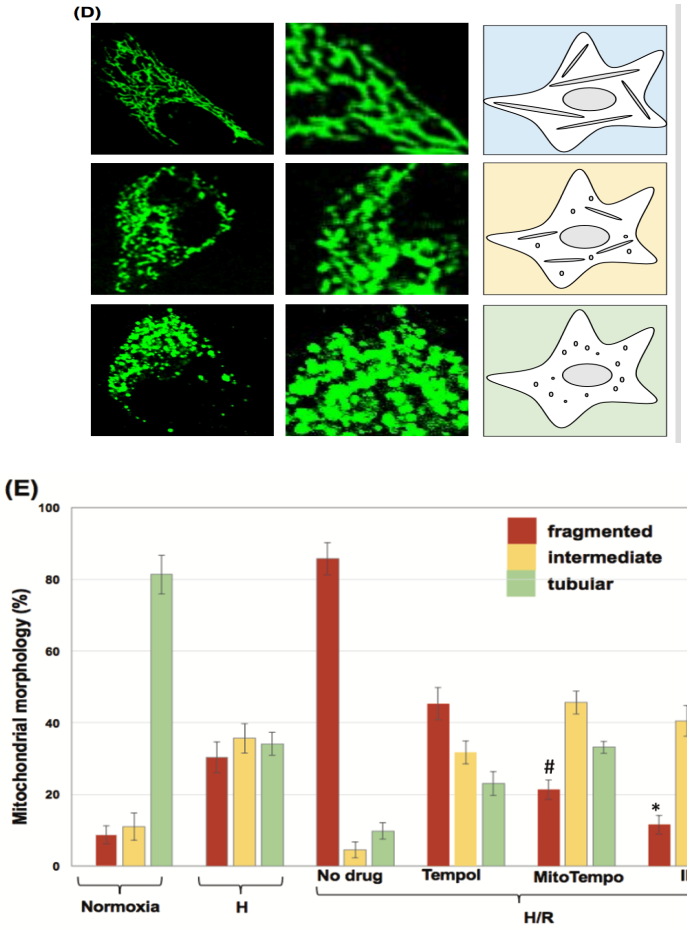

Figure 3. **IPTC** inhibited mitochondrial ROS production and mitochondrial fragmentation in H9C2 cells subjected to hypoxia/reoxygenation (H/R) protocol: (**A**) Representative confocal microscopic images of H9C2 rat cardiomyocytes counter-stained with MitoProbe (100 nM, red fluorescence), MitoTracker (green fluorescence) and Hoechst 33342 (blue fluorescence): Fluorescent images are displayed for cells from a sham-control group (no H/R), cells subjected to hypoxia or cells subjected to H/R with/without drug (Tempol, Mito-Tempo, and **IPTC**) treatment; (**B**) The confocal fluorescence images were pre-processed to improve the quality of binarized images. (**C**) By measuring the mean fluorescence intensity (MFI) of MitoProbe changes in the binarized images, the total ROS generation in the mitochondria was quantified. (**D**) Mitochondrial morphology was categorized as follows: tubular, intermediate, and fragmented. (**E**) Mitochondrial morphology analysis of H9C2 cells subjected to H/R with/without drug (Tempol/Mito-Tempo/IPTC) treatment. Cell were imaged on an inverted laser scanning fluorescent microscope (Olympus) using a 60 x oil immersion objective lens.

During H/R, oxidative stress aggravates lipid peroxidation, DNA damage, and oxidation of proteins. Oxidized lipids and their products are fragmented to produce malondialdehyde (MDA). Next, intracellular levels of MDA (**Figure 4**) were examined. The production of MDA dramatically increased after H/R ($p < 0.01$), whereas Mito-Tempo + H/R ($p < 0.05$) or **IPTC** + H/R treatment significantly reduced the MDA level ($p < 0.05$), suggesting the potential of antioxidant treatment with either Mito-Tempo or **IPTC** for inhibiting lipid peroxidation and oxidative damage induced by H/R protocol.

Preprints (www.preprints.org) | NOT PEER-REVIEWED | Posted: 18 August 2022 doi:10.20944/preprints202208.0352.v1

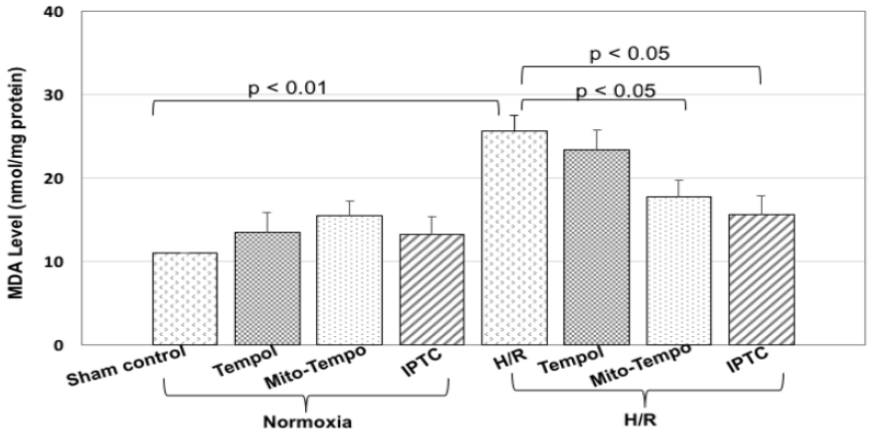

Figure 4. Effect of test compounds (Tempol, Mito-Tempol, and **IPTC**) pretreatment on malondialdehyde (MDA) in H9C2 cells during H/R injury. Values are expressed as mean ± SD; n = 3.

*3.6. **IPTC** induces protective mitophagy against H/R injury:* To carefully monitor the mitophagy response during H/R, H9C2 cells were transfected with GFP-LC3 for labeling autophagosomal membranes. GFP-LC3 puncta can be used to quantitatively analyze autophagosomes. To facilitate the study of the relationship between mitophagy and mtROS production, GFP-LC3 transfected H9C2 cells were further labeled with MitoProbe for real-time monitoring of the colocalization of GFP-LC3 labeling and MitoProbe. In this assay, co-localization of the oxidatively "stressed" mitochondria (visualized by MitoProbe, red fluorescence) with autophagosomes (visualized by GFP-LC3, green fluorescence) provides an estimation of successful fusion between damaged mitochondria with the autophagosomes for trafficking to lysosomes for degradation. Compared to sham control groups (row 1, **Figure 5A**), we found that the percentage of cells with GFP-LC3 punctate increased during the phase of hypoxia (row 2, **Figure 5A**). During the reoxygenation, the percentage of cells with GFP-LC3 punctate remained unchanged. It was noticed that the majority of mitochondria became fragmented accompanied by significantly increased mtROS after reoxygenation (row 3, **Figure 5A**). Interestingly, treatment of H9C2 cells with **IPTC** significantly increased autophagosome formation (visualized by GFP-LC3, green fluorescence) (row 5, **Figure 5A**; see **Figure 5C** for quantitative values). Moreover, the elevated mtROS levels induced by H/R were reduced remarkably after **IPTC** treatment (row 5, **Figure 5A**; see **Figure 5B** for quantitative values). After **IPTC** treatment, most of the oxidatively "stressed" mitochondria (visualized by MitoProbe, red fluorescence) were found to be co-localized with autophagosomes (visualized by GFP-LC3, green fluorescence). The autophagosome-mitochondria fusion results in damaged mitochondria being incorporated into autolysosomes (visualized by double-positive, MitoProbe+/GFP-LC3+, yellow fluorescence), suggesting that the dysfunctional mitochondria are selectively delivered for autophagic degradation (mitophagy).

*3.7. **IPTC** inhibits mPTP opening during hypoxia/reoxygenation (H/R).* The opening of mitochondrial permeability transition pore (mPTP) in H9C2 rat cardiomyoblasts was then evaluated using calcein-AM assay (calcein-AM, AM = acetoxymethyl). During hypoxia (row 2, **Figure 6**), calcein fluorescence in most subcellular compartments was quenched except within the mitochondrial matrix because the intact inner mitochondrial membrane is Co^{2+} impermeable. During the late stage of reoxygenation (row 3, **Figure 6**), the mitochondrial calcein fluorescence was also quenched because of the opening of the mPTP. By contrast, the mitochondrial calcein fluorescence was significantly higher in the rapamycin + H/R (row 4, **Figure 6**) or **IPTC** + H/R-treated cells (row 5, **Figure 6**) than that of the H/R alone-treated cells, indicating that rapamycin/**IPTC** could inhibit the opening of mPTP.

Preprints (www.preprints.org) | NOT PEER-REVIEWED | Posted: 18 August 2022 doi:10.20944/preprints202208.0352.v1

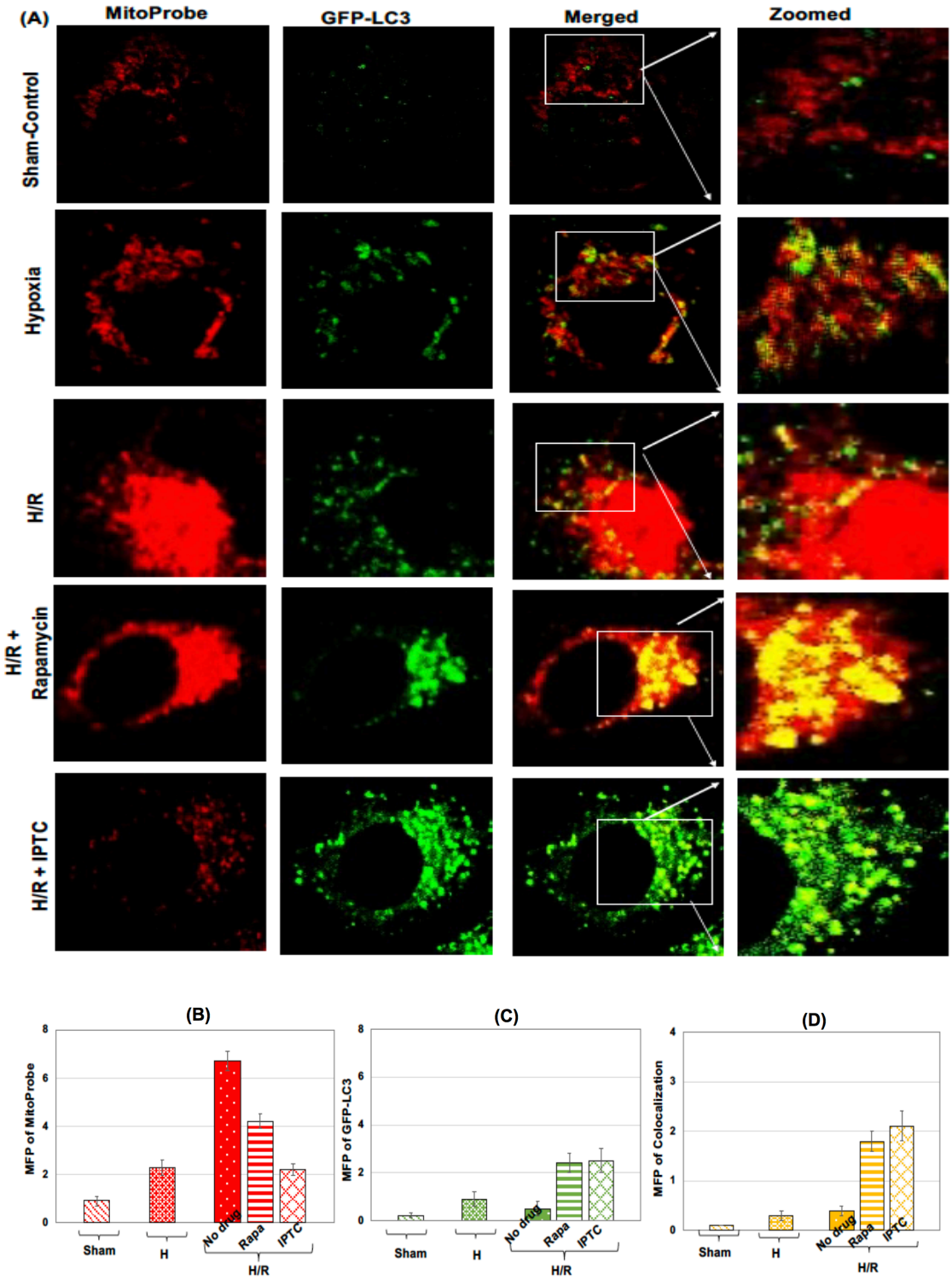

Figure 5. IPTC enhances mitophagy in H9C2 rat cardiomyocytes subjected to hypoxia/reoxygenation (H/R). (A) Representative confocal fluorescent images of rat cardiomyocytes H9C2 subjected to different treatment protocols during H/R. (**B**) mitochondrial ROS level was determined by measuring the mean fluorescence intensity (MFI) of MitoProbes; (**C**) autophagosome formation was estimated by measuring the MFI of GFP-LC3 changes; and (**D**) the co-localization index, estimating mitophagy activity, was produced by measuring the MFI of double-positive (GFP-LC3+/ MitoProbe+) cells with yellow fluorescence. Cell were imaged on an inverted laser scanning fluorescent microscope (Olympus) using a 60 x oil immersion objective lens.

Preprints (www.preprints.org) | NOT PEER-REVIEWED | Posted: 18 August 2022 doi:10.20944/preprints202208.0352.v1

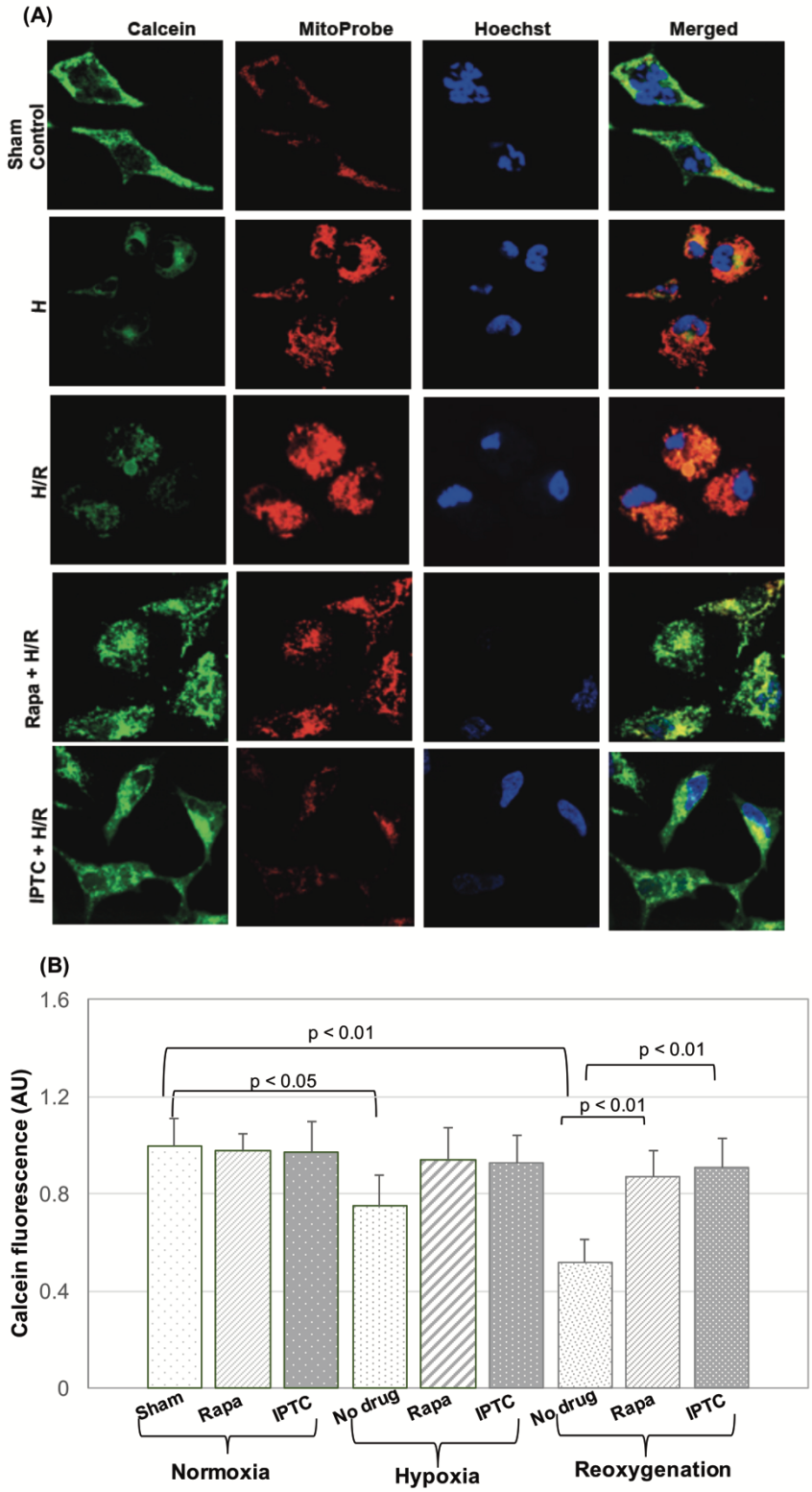

Figure 6. **IPTC inhibits mPTP opening during hypoxia/reoxygenation (H/R)**. (**A**) Representative confocal microscopic images of H9C2 rat cardiomyocytes after incubation with calcein-AM (1 μM, green fluorescence), Co^{2+} (1 mM) and MitoProbe (1 μM, red fluorescence), and Hoechst 33342 (blue fluorescence): Fluorescent images are displayed for cells from a sham-control group (no H/R), cells subjected to hypoxia (H), or cells subjected to H/R with/without rapamycin/**IPTC** treatment; Cell were imaged on an inverted laser scanning fluorescent microscope (Olympus) using a 60 x oil immersion objective lens. (**B**) Quantification of mitochondrial calcein fluorescence in H9C2 cardiomyocytes subjected to H/R in the absence/presence of rapamycin/**IPTC**.

 doi:10.20944/preprints202208.0352.v1

4. Discussion

Under normal physiological conditions, the mitochondrial reactive oxygen species (mtROS) scavenging system keeps mtROS at low levels, the latter serving as intracellular signaling molecules [43]. Under pathophysiological conditions, dysregulated mitochondrial scavenging systems will lead to ROS overproduction and ensuant oxidative damage [43-45]. ROS and oxidative damage are involved in pathological processes of cardiovascular diseases (CVDs). Traditionally, free radicals were merely considered toxins that induce oxidative stress and concomitant cellular damage. For decades, considerable research has been focused on eliminating excess free radicals generated in the body. Yet, experimental and clinical studies focused on the use of antioxidant therapy to mitigate myocardial damage have yielded mixed results. Moreover, decreasing the systemic level of ROS by using antioxidant therapy may be detrimental in certain instances.

β-carbolines are biologically active alkaloids, and these compounds have been reported to possess a wide range of biological effects, such as anti-inflammatory, antithrombotic activities, antivirus, anticancer and free radical scavenging activities [46]. Previous studies demonstrated the potential application of β-carboline derivatives in the treatment of cardiovascular diseases like hypertension [47], myocardial infarction [25], [48], cancer [49-52], and ischemia/reperfusion injury [53-59]. In addition, 4-hydroxy-2,2,6,6-tetramethyl-piperidine-N-oxyl (Tempol) has gained attention. It has been suggested that the antioxidant capacity of Tempol is structurally related because it is a stable nitroxide radical compound [60]. Additionally, Tempol's antioxidant capacity is likely enhanced because it possesses superoxide dismutase (SOD)-mimicking activity [60]. In our present study, we have demonstrated that **IPTC** exhibits superior free radical scavenging activity toward •NO, •OH, and H_2O_2 in the PC12 cell survival assay (**Table 1**). The elimination of the free radicals is critical for alleviating oxidative damage. Incubating cells with the **IPTC** could improve the PC12 cell viability, suggesting that **IPTC** has a good radical scavenging potential toward different kinds of free radical species. Compared to Tempol or compound **4** (the precursor of **IPTC**), **IPTC** seems to have better free radical scavenging activity, and this is likely due to the synergetic effects of these two seemingly irrelevant antioxidant moieties, β-carboline and nitroxide.

Because of its free radical scavenging potentials toward different free radicals, especially toward •NO, one may question whether **IPTC** may serve as a pro-thrombotic agent. Previously, we reported the antithrombotic properties of a series of phenolic tetrahydro-β-carboline RGD peptide conjugates [61]. Recently, we examined the effect of **IPTC** on platelet activation induced by the physiologic agonists, ADP and PAF. We found that **IPTC** could inhibit platelet activation and aggregation induced by ADP and PAF in a dose-dependent manner and the results will be published elsewhere. The exact action mechanism of **IPTC** in regulating platelet activity remains unclear. We hypothesize that the antiplatelet aggregation activity of **IPTC** is likely through the balance of autophagy and the maintenance of optimal platelet intracellular ROS levels.

Encouraged by these results, we further examined the effect of **IPTC** on mitochondrial morphology and mitochondrial oxidative status using rat cardiomyocytes H9C2 in a hypoxia/reoxygenation (H/R) cellular model. H9C2 cells closely mimic primary cardiomyocytes in terms of energy metabolism and are sensitive to H/R [63]. To provide better mechanistic insight that cannot be obtained from a clinical situation, a simplified cellular model is adopted. Cardiomyocytes can be used as a powerful *in vitro* model of ischemia-reperfusion (I/R), whereby ischemia is simulated with hypoxia and reperfusion with reoxygenation. By eliminating the influences of other cell types (e.g., fibroblasts, endothelial cells, inflammatory/immune cells, and plates) or circulating factors (e.g., hormones, neurotransmitters, and cytokines), this model system allows us precise control of the cellular and extracellular environment, especially the impact of H/R on cardiomyocytes [64]. Moreover, it allows us to directly compare the efficacy of the tested compounds. The H/R model is commonly used in ischemia research that may be combined with other injury

 doi:10.20944/preprints202208.0352.v1

models to fully reproduce features of I/R injury [64]. In our present study, the culture medium was replaced with DMEM containing no glucose before the induction of hypoxia.

To monitor mitochondrial ROS production during H/R, H9C2 cells were labeled with MitoProbe (a fluorogenic dye that is highly sensitive for monitoring mtROS [33-39]). Through measurement of the MFI of MitoProbe at different time points of H/R, the total amount of mtROS could be estimated. Simultaneously, MitoTracker is used to gauge alterations of mitochondrial morphology. We observed an ~2.5- fold increase in mitochondrial ROS levels during the phage of hypoxia. As shown in **Figure 3A&C**, an ~7.4- fold elevation of ROS in the mitochondria was associated with the phage of reoxygenation, a highly toxic environment for H9C2 cells. We observed significant inhibition of mtROS with the administration of Mito-Tempol or **IPTC** in our cell model.

During reoxygenation, the number of cells with intermediate and fragmented mitochondria increased significantly. Hypoxia was found to significantly increase the percentage of cells with intermediate or fragmented mitochondria when compared to the sham-control cells, whereas reoxygenation resulted in most cells displaying fragmented mitochondria. During H/R, the percentage of sham-control cells exhibiting long tubular mitochondria, and the mitochondria with the intermediate as well as the fragmented morphology were predominantly aggregated in the perinuclear region. Pretreatment of cells with **IPTC** resulted in significant protection during H/R and attenuated the fragmented mitochondrial appearance. The H9C2 cells treated with **IPTC** + H/R exhibited an increase in the percentage of cells with tubular mitochondria (**Figure 3E**). The damage to the cardiac H9C2 cells induced by the H/R protocol may be due to, in part, the overproduction of ROS and the accumulation of the damaged mitochondria. The H/R-induced ROS overproduction is accompanied by the reduction of endogenous antioxidants. We further demonstrated that cardiomyocytes H9C2 subjected to H/R caused a marked reduction of cell viability and elevation of oxidative stress accompanied by LDH release and MDA production.

Unlike Tempol, whose $t_{1/2}$ in the blood is only 15 s with only narrow nitroxide antioxidant capacity [70], the antioxidant activity of **IPTC** may not only originate from the nitroxide moiety of Tempol but also from the β-carboline moiety of **IPTC**, which would coordinately enhance the radical-scavenging capacity of nitroxide while increasing the half-life of the molecule. The hydrophobic microenvironments induced by β-carboline's planar tricyclic system and the hydrophilic nature of the side chain of the RGDS peptide are likely to contribute to the enhanced overall antioxidant-scavenging property of **IPTC**. Based on the predicted lowest energy conformation of **IPTC**, we speculate that a nitroxide radical surrounded by hydrophobic and resonance-stabilized amino acid side chains may result in enhanced bioavailability that correlates to improved scavenging of •OH or NO• and associated cytoprotective effects.

One of the primary factors in initiating the pathological response to the I/R injury is the overproduction of ROS in the mitochondria. The increase of mtROS during reoxygenation contributes to the progression of cardiomyocyte death. As cardiomyocytes are post-mitotic cells with high demands for energy, they are rich in mitochondria and are particularly susceptible to damaged and dysfunctional mitochondria. The alterations of mitochondrial morphology have been associated with several fundamental cellular functions [64]. H/R induces "excessive" fragmentation of mitochondria, which is an important sign of the initiation of apoptosis. The aggregates of fragmented mitochondria can continuously produce ROS and trigger a series of damaging events eventually leading to cell death. Removal of dysfunctional mitochondria is the key to cellular survival.

Autophagy is a cellular self-protective mechanism. In our present study, GFP-LC3 fluorescence was used to study autophagy in H9C2 cells. During the early phase of H/R, the number of GFP-LC3 labeled structures (GFP-LC3 green "dots"), representing autophagosomes, was increased in cells exposed to hypoxia, suggesting autophagy is activated. Furthermore, we evaluated the co-localization of MitoProbe-positive (representing oxidatively "stressed" mitochondria) and GFP-LC3-positive puncta (representing autophago-

Preprints (www.preprints.org) | NOT PEER-REVIEWED | Posted: 18 August 2022 doi:10.20944/preprints202208.0352.v1

somes). Compared to the normoxia group, the cells exposed to hypoxia exhibited an increased co-localization of MitoProbe- and GFP-LC3-positive puncta, suggesting activated autophagy could effectively remove the oxidatively damaged mitochondria. Although the mitochondrial ROS levels increased by ~2.5 fold, it is still in a tolerable range for H9C2 cells. When oxygen and nutrients are resumed to normal condition, the number of oxidatively "stressed" mitochondria increased significantly. However, the percentage of colocalization of MitoProbe- and GFP-LC3-positive puncta remains relatively low (**Figure 5**), suggesting the degradation capacity of mitophagy machinery may be impaired during reoxygenation. Defective mitophagy triggers the accumulation of damaged mitochondria causing a sudden upsurge of mtROS levels (~7.4-fold increase), which may further induce mitochondrial permeability transition pore (mPTP) opening (**Figure 6**). Pretreatment with **IPTC** led to a dramatically increased colocalization of yellow puncta [double positive, MitoProbe+ (red fluorescence)/GFP-LC3+ (green fluorescence)] per cell in H9C2 cardiomyocytes (row 5, **Figure 5A**), suggesting that mitophagy is activated after **IPTC** treatment. Thus, the ROS-producing mitochondria could be effectively removed thereby protecting cells against further damage induced by H/R. **IPTC**-pretreated cells revealed a level of mitophagy comparable to that of rapamycin-treated cells (row 4, **Figure 5A**).

Autophagy has been recognized as an important cell survival process in the experimental model of cardiac I/R injury. However, following acute ischemic injuries, basal levels of autophagy may be overwhelmed, which may eventually lead to cardiomyocyte death. It is important to identify specific chemical modulators of autophagy that can be used to modulate autophagy *in vivo*. Rapamycin has been reported to enhance mitophagy and reduce apoptosis after spinal I/R injury [66]. In addition, it has been reported that spermidine could promote autophagy through the AMPK/mTOR pathway thereby alleviating myocardial injury. Interestingly, spermidine's anti-oxidative stress and anti-inflammatory properties also contribute to the reduction of cardiac dysfunction induced by myocardial infarction [67]. Because of the complex interplay between ROS signaling and autophagy modulators [68] [69] in AMI, identification of the optimal combination of autophagy modulators and antioxidants to improve cardiac function after AMI remains a challenge. In our present study, we demonstrated that **IPTC**-pretreated cardiac cells could significantly inhibit mPTP opening, a process that is critical in reperfusion injury and heart failure. This unique feature is likely achieved by its dual function (a combined modulation of autophagy and ROS production). When **IPTC** is incubated with cells, a dynamic equilibrium is established between the three forms of **IPTC** that is highly dependent on the cellular "redox status". The reduction rates of IPTC-NO• in normal and inflammatory cells differ because their redox statuses are quantitatively different. In hypoxic inflammatory cells, the nitroxide form (IPTC-NO•) is rapidly reduced to its corresponding hydroxylamine form (IPTC-NOH). In oxygen-rich normal cells (i.e. cardiomyocytes), the nitroxide moiety of **IPTC** remains in the oxidized form (IPTC-NO•).

Our *in vitro* studies provide further evidence that cytoprotection associated with **IPTC** may correlate with its dual function (antioxidant and mitophagy-inducing potential), which originates from the unique kinetic equilibrium capacities of its three forms, the nitroxide form (IPTC-NO•), oxoammonium pair (IPTC-$\overset{\oplus}{N}O$) and hydroxylamine form (IPTC-NOH). In theory, the unique self-replenish property of **IPTC** can enable cells never run out of antioxidants. The cellular redox process can be continuously balanced via reversible one-electron transfer reactions. Thus, under redox-balanced microenvironment, the mitochondria can constantly undergo damage repair, whereas severely damaged mitochondria will be degraded and recycled by **IPTC**-triggered mitophagy. Our proposed molecular mechanism of **IPTC** is presented graphically in **Figure 7.** Currently, we are working on transitioning these *in vitro* studies to the examination of the cardioprotective effect of **IPTC** in an *in vivo* model of myocardial I/R injury.

Preprints (www.preprints.org) | NOT PEER-REVIEWED | Posted: 18 August 2022 doi:10.20944/preprints202208.0352.v1

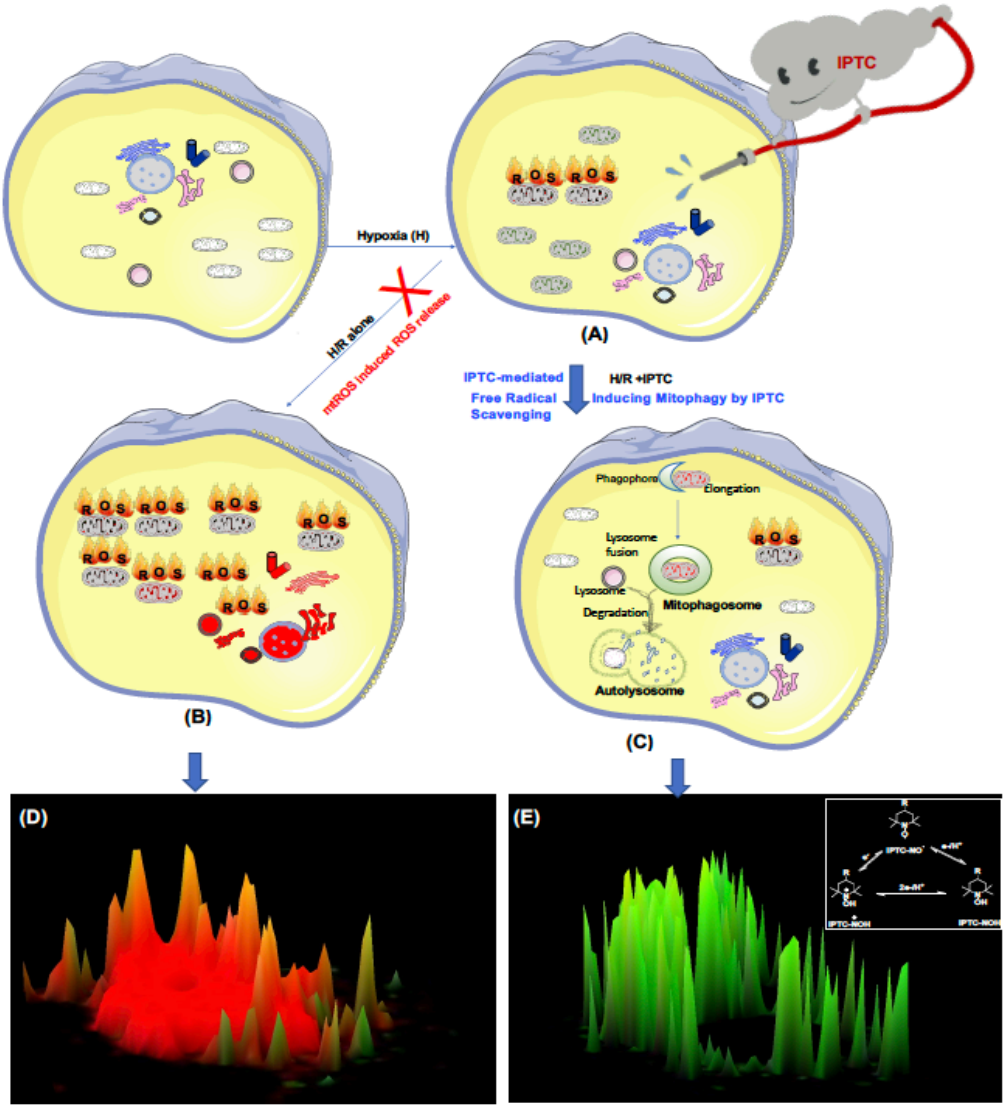

Figure 7. IPTC can put out a "fire" in the heart mitochondria. The initial mtROS generated during hypoxia (**A**) can induce neighboring mitochondria to release more ROS (**B**), the so-called "ROS triggered ROS to release". Thus, vast mitochondrial damage overwhelms autophagosomes and their capacity to remove damaged mitochondria. During hypoxia/reoxygenation (H/R), nitroxide metabolism occurs constantly via the reduction of the nitroxide form (IPTC-NO•) to hydroxylamine (IPTC-NOH). IPTC-NO•, having a single unpaired electron, can continuously undergo redox transformations between the one-electron oxidized state, the oxoammonium cation (IPTC-$\overset{\oplus}{N}O$), and the one-electron reduced IPTC-NOH. Under the balanced redox microenvironment (**C**), the mitochondria undergo constant damage repair through mitochondrial dynamics, whereas severely damaged mitochondria will be degraded and recycled through **IPTC**-induced mitophagy. 3D surface plot of the mitochondria of the cardiac cells co-stained with MitoProbe (red fluorescence) and MitoTracker (green fluorescence) subjected to H/R in the absence (**D**) and presence **(E)** of **IPTC**.

5. Conclusions

Pre-treatment with a novel multifunctional agent, **IPTC**, was found to ameliorate increased ROS levels and weakened mitophagy induced by H/R, suggesting induction of mitophagy in an adaptive manner that may mitigate mitochondrial oxidative stress. We propose that the protective effects of **IPTC** originate from a synergistic effect between mitophagy maintenance combined with the capacity to maintain homeostasis of mitochon-

drial ROS contents. Our study presents a novel molecular approach that synergizes autophagy with mitochondrial function to prevent ischemic/reperfusion damage to cardiomyocytes.

Author Contributions: Conceptualization, K.G.M. and L.B.; methodology and investigation, L.B.; X.G.; X.Y. S.H.; S.J.; X.G.; X.Y.; S. J., and K.G.M. data analysis, L.B.; X.G.; X.Y.; S. H.; S. J., and K.G.M. writing, reviewing and editing; L.B.; funding acquisition. All authors have read and agreed to the published version of the manuscript.

Funding: This research was funded by American Heart Association (AHA), grant number (1807047).

Acknowledgments: We thank the American Heart Association (AHA grant #1807047) for the support of this project. The authors are particularly thankful to Dr. David Hemmer for his ongoing support of our work.

Conflicts of Interest: The authors declare no conflict of interest.

References

1. Heusch G. Myocardial ischaemia-reperfusion injury and cardioprotection in perspective. Nat Rev Cardiol. 2020 Dec;17(12):773-789. doi: 10.1038/s41569-020-0403-y. Epub 2020 Jul 3. PMID: 32620851.

2. Rout A, Tantry US, Novakovic M, Sukhi A, Gurbel PA. Targeted pharmacotherapy for ischemia reperfusion injury in acute myocardial infarction. Expert Opin Pharmacother. 2020 Oct;21(15):1851-1865. doi: 10.1080/14656566.2020.1787987. Epub 2020 Jul 13. PMID: 32659185.

3. Bugger H, Pfeil K. Mitochondrial ROS in myocardial ischemia reperfusion and remodeling. Biochim Biophys Acta Mol Basis Dis. 2020 Jul 1;1866(7):165768. doi: 10.1016/j.bbadis.2020.165768. Epub 2020 Mar 12. PMID: 32173461.

4. Verstraete M, Zoldhelyi P. Novel antithrombotic drugs in development. Drugs. 1995 Jun;49(6):856-84. doi: 10.2165/00003495-199549060-00002. PMID: 7641602.

5. Nicholson NS, Panzer-Knodle SG, Salyers AK, Taite BB, King LW, Miyano M, Gorczynski RJ, Williams MH, Zupec ME, Tjoeng FS, et al. In vitro and in vivo effects of a peptide mimetic (SC-47643) of RGD as an antiplatelet and antithrombotic agent. Thromb Res. 1991 Jun 1;62(5):567-78. doi: 10.1016/0049-3848(91)90029-v. PMID: 1896969.

6. Wilcox CS. Effects of tempol and redox-cycling nitroxides in models of oxidative stress. Pharmacol Ther. 2010 May;126(2):119-45. doi: 10.1016/j.pharmthera.2010.01.003. Epub 2010 Feb 11. PMID: 20153367; PMCID: PMC2854323.

7. Simonsen U, Christensen FH, Buus NH. The effect of tempol on endothelium-dependent vasodilatation and blood pressure. Pharmacol Ther. 2009 May;122(2):109-24. Epub 2009 Mar 5. PMID: 19268689.

8. Dornas WC, Silva M, Tavares R, de Lima WG, dos Santos RC, Pedrosa ML, Silva ME. Efficacy of the superoxide dismutase mimetic tempol in animal hypertension models: a meta-analysis. J Hypertens. 2015 Jan;33(1):14-23.

9. Wilcox CS, Pearlman A. Chemistry and antihypertensive effects of tempol and other nitroxides. Pharmacol Rev. 2008 Dec;60(4):418-69. doi: 10.1124/pr.108.000240. PMID: 19112152; PMCID: PMC2739999.

10. Li JY, Sun XF, Li JJ, Yu F, Zhang Y, Huang XJ, Jiang FX. The antimalarial activity of indole alkaloids and hybrids. Arch Pharm (Weinheim). 2020 Nov;353(11):e2000131. doi: 10.1002/ardp.202000131. Epub 2020 Aug 12. PMID: 32785974.

11. Zhang L, Li D, Yu S. Pharmacological effects of harmine and its derivatives: a review. Arch Pharm Res. 2020 Dec;43(12):1259-1275. doi: 10.1007/s12272-020-01283-6. Epub 2020 Nov 18. PMID: 33206346.

12. Munir S, Shahid A, Aslam B, Ashfaq UA, Akash MSH, Ali MA, Almatroudi A, Allemailem KS, Rajoka MSR, Khurshid M. The Therapeutic Prospects of Naturally Occurring and Synthetic Indole Alkaloids for Depression and Anxiety Disorders. Evid Based Complement Alternat Med. 2020 Oct 16;2020:8836983. doi: 10.1155/2020/8836983. PMID: 33123212; PMCID: PMC7585661.

13. Liu Y, Cui Y, Lu L, Gong Y, Han W, Piao G. Natural indole-containing alkaloids and their antibacterial activities. Arch Pharm (Weinheim). 2020 Oct;353(10):e2000120. doi: 10.1002/ardp.202000120. Epub 2020 Jun 18. PMID: 32557757.

14. Ayipo YO, Mordi MN, Mustapha M, Damodaran T. Neuropharmacological potentials of β-carboline alkaloids for neuropsychiatric disorders. Eur J Pharmacol. 2021 Feb 15;893:173837. doi: 10.1016/j.ejphar.2020.173837. Epub 2020 Dec 25. PMID: 33359647.

15. Mitra S, Prova SR, Sultana SA, Das R, Nainu F, Emran TB, Tareq AM, Uddin MS, Alqahtani AM, Dhama K, Simal-Gandara J. Therapeutic potential of indole alkaloids in respiratory diseases: A comprehensive review. Phytomedicine. 2021 Sep;90:153649. doi: 10.1016/j.phymed.2021.153649. Epub 2021 Jul 15. PMID: 34325978.

16. Zhu Y, Zhao J, Luo L, Gao Y, Bao H, Li P, Zhang H. Research progress of indole compounds with potential antidiabetic activity. Eur J Med Chem. 2021 Jun 23;223:113665. doi: 10.1016/j.ejmech.2021.113665. Epub ahead of print. PMID: 34192642.

17. Mauger A, Jarret M, Kouklovsky C, Poupon E, Evanno L, Vincent G. The chemistry of mavacurane alkaloids: a rich source of bis-indole alkaloids. Nat Prod Rep. 2021 Mar 5. doi: 10.1039/d0np00088d. Epub ahead of print. PMID: 33666614.

18. Pozzi E, Fumagalli G, Chiorazzi A, Canta A, Cavaletti G. Genetic factors influencing the development of vincristine-induced neurotoxicity. Expert Opin Drug Metab Toxicol. 2021 Feb;17(2):215-226. doi: 10.1080/17425255.2021.1855141. Epub 2020 Dec 6. PMID: 33283553.

19. La X, Zhang L, Li Z, Yang P, Wang Y. Berberine-induced autophagic cell death by elevating GRP78 levels in cancer cells. *Oncotarget*. 2017;8(13):20909-20924.

20. Park MK, Rhee YH, Lee HJ, Lee EO, Kim KH, Park MJ, Jeon BH, Shim BS, Jung CH, Choi SH, Ahn KS, Kim SH. Antiplatelet and antithrombotic activity of indole-3-carbinol in vitro and in vivo. Phytother Res. 2008 Jan;22(1):58-64. doi: 10.1002/ptr.2260. PMID: 17724769.

21. De Santi M, Galluzzi L, Lucarini S, Paoletti MF, Fraternale A, Duranti A, De Marco C, Fanelli M, Zaffaroni N, Brandi G, Magnani M. The indole-3-carbinol cyclic tetrameric derivative CTet inhibits cell proliferation via overexpression of p21/CDKN1A in both estrogen receptor-positive and triple-negative breast cancer cell lines. Breast Cancer Res. 2011 Mar 24;13(2):R33. doi: 10.1186/bcr2855. PMID: 21435243; PMCID: PMC3219196.

22. Peyvandi F, Garagiola I, Baronciani L. Role of von Willebrand factor in the haemostasis. *Blood Transfus*. 2011;9 Suppl 2(Suppl 2):s3-s8. doi:10.2450/2011.002S.

23. Bi W, Li X, Bi Y, Xue P, Zhang Y, Gao X, Wang Z, Li M, Itagaki Y, Bi L. Novel TEMPO-PEG-RGDs conjugates remediate tissue damage induced by acute limb ischemia/reperfusion. J. Med. Chem. 2012 May 10;55(9):4501-5. doi: 10.1021/jm201381w. Epub 2012 Apr 23. PMID: 22439897.

24. Bi W, Bi L, Cai J, Liu S, Peng S, Fischer NO, Tok JB, Wang G. Dual-acting agents that possess free radical scavenging and antithrombotic activities: design, synthesis, and evaluation of phenolic tetrahydro-beta-carboline RGD peptide conjugates. Bioorg Med Chem Lett. 2006 Sep 1;16(17):4523-7. doi: 10.1016/j.bmcl.2006.06.024. Epub 2006 Jun 23. PMID: 16797986.

25. Bi W, Cai J, Liu S, Baudy-Floc'h M, Bi L. Design, synthesis and cardioprotective effect of a new class of dual-acting agents: phenolic tetrahydro-beta-carboline RGD peptidomimetic conjugates. Bioorg Med Chem. 2007 Nov 15;15(22):6909-19. doi: 10.1016/j.bmc.2007.08.022. Epub 2007 Aug 21. PMID: 17827017.

26. Bi W, Bi Y, Gao X, Yan X, Zhang Y, Xue P, Bammert CE, Legalley TD, Michael Gibson K, Bi L, Wang JX. Anti-inflammatory, analgesic and antioxidant activities of novel kyotorphin-nitroxide hybrid molecules. Bioorg Med Chem Lett. 2016 Apr 15;26(8):2005-13. doi: 10.1016/j.bmcl.2016.02.086. Epub 2016 Mar 3. PMID: 26961795.

27. Bi W, Bi Y, Gao X, Yan X, Zhang Y, Harris J, Legalley TD, Gibson KM, Bi L. Pharmacological protection of mitochondrial function mitigates acute limb ischemia/reperfusion injury. Bioorg Med Chem Lett. 2016 Aug 15;26(16):4042-51. doi: 10.1016/j.bmcl.2016.06.079. Epub 2016 Jun 28. PMID: 27390069.

28. Bi W, Bi Y, Xue P, Zhang Y, Gao X, Wang Z, Li M, Baudy-Floc'h M, Ngerebara N, Gibson KM, Bi L. A new class of β-carboline alkaloid-peptide conjugates with therapeutic efficacy in acute limb ischemia/reperfusion injury. Eur J Med Chem. 2011 May;46(5):1453-62. doi: 10.1016/j.ejmech.2011.01.021. Epub 2011 Jan 21.

29. Bi W, Cai J, Xue P, Zhang Y, Liu S, Gao X, Li M, Wang Z, Baudy-Floc'h M, Green SA, Bi L. Protective effect of nitronyl nitroxide-amino acid conjugates on liver ischemia-reperfusion induced injury in rats. Bioorg Med Chem Lett. 2008 Mar 15;18(6):1788-94. doi: 10.1016/j.bmcl.2008.02.030. Epub 2008 Feb 16.

30. Lahiani A, Brand-Yavin A, Yavin E, Lazarovici P. Neuroprotective Effects of Bioactive Compounds and MAPK Pathway Modulation in "Ischemia"-Stressed PC12 Pheochromocytoma Cells. Brain Sci. 2018 Feb 8;8(2):32. doi: 10.3390/brainsci8020032. PMID: 29419806; PMCID: PMC5836051.

31. Yapici NB, Jockusch S, Moscatelli A, Mandalapu SR, Itagaki Y, Bates DK, Wiseman S, Gibson KM, Turro NJ, Bi L. New rhodamine nitroxide based fluorescent probes for intracellular hydroxyl radical identification in living cells. Org Lett. 2012 Jan 6;14(1):50-3. doi: 10.1021/ol202816m. Epub 2011 Dec 16. PMID: 22176578.

32. Mosmann T. Rapid colorimetric assay for cellular growth and survival: application to proliferation and cytotoxicity assays. J Immunol Methods. 1983 Dec 16;65(1-2):55-63. doi: 10.1016/0022-1759(83)90303-4. PMID: 6606682.

33. Bi, L., Mitochondria-Targeting Probes. (PCT/US2013/055578; WO2014/058535).

34. Yapici NB, Mandalapu S, Gibson KM, Bi L. Targeted fluorescent probes for detection of oxidative stress in the mitochondria. Bioorg Med Chem Lett. 2015 Sep 1;25(17):3476-80. doi: 10.1016/j.bmcl.2015.07.011. Epub 2015 Jul 9. PMID: 26189896.

35. Yapici NB, Bi Y, Li P, Chen X, Yan X, Mandalapu SR, Faucett M, Jockusch S, Ju J, Gibson KM, Pavan WJ, Bi L. Highly stable and sensitive fluorescent probes (LysoProbes) for lysosomal labeling and tracking. Sci Rep. 2015 Feb 26;5:8576. doi: 10.1038/srep08576. PMID: 25715948; PMCID: PMC4341211.

36. Chen X, Bi Y, Wang T, Li P, Yan X, Hou S, Bammert CE, Ju J, Gibson KM, Pavan WJ, Bi L. Lysosomal targeting with stable and sensitive fluorescent probes (Superior LysoProbes): applications for lysosome labeling and tracking during apoptosis. Sci Rep. 2015 Mar 11;5:9004. doi: 10.1038/srep09004. PMID: 25758662; PMCID: PMC4355733.

37. Bi W, Bi Y, Gao X, Li P, Hou S, Zhang Y, Bammert C, Jockusch S, Legalley TD, Michael Gibson K, Bi L. Indole-TEMPO conjugates alleviate ischemia-reperfusion injury via attenuation of oxidative stress and preservation of mitochondrial function. Bioorg Med Chem. 2017 May 1;25(9):2545-2568. doi: 10.1016/j.bmc.2017.03.033. Epub 2017 Mar 19. PMID: 28359673.

38. Bi W, Bi Y, Li P, Hou S, Yan X, Hensley C, Bammert CE, Zhang Y, Gibson KM, Ju J, Bi L. Indole Alkaloid Derivative B, a Novel Bifunctional Agent That Mitigates 5-Fluorouracil-Induced Cardiotoxicity. ACS Omega. 2018 Nov 30;3(11):15850-15864. doi: 10.1021/acsomega.8b02139. Epub 2018 Nov 21. PMID: 30533582; PMCID: PMC6275955.

39. Bi W, Bi Y, Li P, Hou S, Yan X, Hensley C, Zhang Y, Jockusch S.; Legalley, T. D.; Gibson KM, Bi L. Cardioprotection Effects of LPTC-5 Involve Mitochondrial Protection and Dynamics. ACS Omega 2019, 4, 6, 9868-9877.

40. Trnka J., Blaikie F.H., Logan A., Smith R.A., Murphy M.P. Antioxidant properties of MitoTEMPOL and its hydroxylamine. Free Radic. Res. 2009;43(1):4–12.

41. Sarkar S, Ravikumar B, Floto RA, Rubinsztein DC. Rapamycin and mTOR-independent autophagy inducers ameliorate toxicity of polyglutamine-expanded huntingtin and related proteinopathies. Cell Death Differ. 2009 Jan;16(1):46-56. doi: 10.1038/cdd.2008.110. Epub 2008 Jul 18. PMID: 18636076.

42. Mironov SL, Ivannikov MV, Johansson M. [Ca2+]i signaling between mitochondria and endoplasmic reticulum in neurons is regulated by microtubules. From mitochondrial permeability transition pore to Ca2+-induced Ca2+ release. J Biol Chem. 2005 Jan 7;280(1):715-21. doi: 10.1074/jbc.M409819200. Epub 2004 Oct 29. PMID: 15516333.

43. Giorgi C, Marchi S, Simoes ICM, et al. Mitochondria and Reactive Oxygen Species in Aging and Age-Related Diseases. *Int Rev Cell Mol Biol*. 2018;340:209-344. doi:10.1016/bs.ircmb.2018.05.006

44. Vásquez-Trincado C, García-Carvajal I, Pennanen C, et al. Mitochondrial dynamics, mitophagy and cardiovascular disease. *J Physiol*. 2016;594(3):509-525. doi:10.1113/JP271301

45. Yao Z, Tong J, Tan X, Li CQ, Shao A, Kin WC. Vanden Hoek TL, Becker LB, Head CA, and Schumacker PT. Role of reactive oxygen species in acetylcholine-induced preconditioning in cardiomyocytes. Am J Physiol Heart Circ Physiol 277: H2504–H2509, 1999.

46. Ježek J, Cooper KF, Strich R. Reactive Oxygen Species and Mitochondrial Dynamics: The Yin and Yang of Mitochondrial Dysfunction and Cancer Progression. *Antioxidants (Basel)*. 2018;7(1):13. Published 2018 Jan 16. doi:10.3390/antiox7010013.

47. Piechowska P, Zawirska-Wojtasiak R, Mildner-Szkudlarz S. Bioactive β-Carbolines in Food: A Review. Nutrients. 2019 Apr 11;11(4):814. doi: 10.3390/nu11040814. PMID: 30978920; PMCID: PMC6520841.

48. Galiè N, Barberà JA, Frost AE, Ghofrani HA, Hoeper MM, McLaughlin VV, Peacock AJ, Simonneau G, Vachiery JL, Grünig E, Oudiz RJ, Vonk-Noordegraaf A, White RJ, Blair C, Gillies H, Miller KL, Harris JH, Langley J, Rubin LJ; AMBITION Investigators. Initial Use of Ambrisentan plus Tadalafil in Pulmonary Arterial Hypertension. N Engl J Med. 2015 Aug 27;373(9):834-44. doi: 10.1056/NEJMoa1413687. PMID: 26308684.

49. Zhang H, Zhang RH, Liao XM, Yang D, Wang YC, Zhao YL, Xu GB, Liu CH, Li YJ, Liao SG, Zhou M. Discovery of β-Carboline Derivatives as a Highly Potent Cardioprotectant against Myocardial Ischemia-Reperfusion Injury. J Med Chem. 2021 Jul 8;64(13):9166-9181. doi: 10.1021/acs.jmedchem.1c00384. Epub 2021 Jun 16. PMID: 34132541.

50. Panice MR, Lopes SMM, Figueiredo MC, Goes Ruiz ALT, Foglio MA, Nazari Formagio AS, Sarragiotto MH, Pinho E Melo TMVD. New 3-tetrazolyl-β-carbolines and β-carboline-3-carboxylates with anti-cancer activity. Eur J Med Chem. 2019 Oct 1;179:123-132. doi: 10.1016/j.ejmech.2019.05.085. Epub 2019 May 31. PMID: 31247374.

51. Sun J, Wang J, Wang X, Hu X, Cao H, Bai J, Li D, Hua H. Design and synthesis of β-carboline derivatives with nitrogen mustard moieties against breast cancer. Bioorg Med Chem. 2021 Sep 1;45:116341. doi: 10.1016/j.bmc.2021.116341. Epub 2021 Aug 2. PMID: 34365102.

52. Zhao M, Bi L, Wang W, Wang C, Baudy-Floc'h M, Ju J, Peng S. Synthesis and cytotoxic activities of beta-carboline amino acid ester conjugates. Bioorg Med Chem. 2006 Oct 15;14(20):6998-7010. doi: 10.1016/j.bmc.2006.06.021. Epub 2006 Jun 27. PMID: 16806943.

53. Liang J, Zbieg JR, Blake RA, Chang JH, Daly S, DiPasquale AG, Friedman LS, Gelzleichter T, Gill M, Giltnane JM, Goodacre S, Guan J, Hartman SJ, Ingalla ER, Kategaya L, Kiefer JR, Kleinheinz T, Labadie SS, Lai T, Li J, Liao J, Liu Z, Mody V, McLean N, Metcalfe C, Nannini MA, Oeh J, O'Rourke MG, Ortwine DF, Ran Y, Ray NC, Roussel F, Sambrone A, Sampath D, Schutt LK, Vinogradova M, Wai J, Wang T, Wertz IE, White JR, Yeap SK, Young A, Zhang B, Zheng X, Zhou W, Zhong Y, Wang X. GDC-9545 (Giredestrant): A Potent and Orally Bioavailable Selective Estrogen Receptor Antagonist and Degrader with an Exceptional Preclinical Profile for ER+ Breast Cancer. J Med Chem. 2021 Aug 26;64(16):11841-11856. doi: 10.1021/acs.jmedchem.1c00847. Epub 2021 Jul 12. PMID: 34251202.

54. Bi W, Bi Y, Xue P, Zhang Y, Gao X, Wang Z, Li M, Baudy-Floc'h M, Ngerebara N, Li X, Gibson KM, Bi L. Novel β-carboline-tripeptide conjugates attenuate mesenteric ischemia/reperfusion injury in the rat. Eur J Med Chem. 2011 Jun;46(6):2441-52. doi: 10.1016/j.ejmech.2011.03.029. Epub 2011 Mar 21. PMID: 21474215.

55. Bi W, Bi Y, Gao X, Li P, Hou S, Zhang Y, Bammert C, Jockusch S, Legalley TD, Michael Gibson K, Bi L. Indole-TEMPO conjugates alleviate ischemia-reperfusion injury via attenuation of oxidative stress and preservation of mitochondrial function. Bioorg Med Chem. 2017 May 1;25(9):2545-2568. doi: 10.1016/j.bmc.2017.03.033. Epub 2017 Mar 19. PMID: 28359673.

56. Koka S, Das A, Salloum FN, Kukreja RC. Phosphodiesterase-5 inhibitor tadalafil attenuates oxidative stress and protects against myocardial ischemia/reperfusion injury in type 2 diabetic mice. Free Radic Biol Med. 2013 Jul;60:80-8. doi: 10.1016/j.freeradbiomed.2013.01.031. Epub 2013 Feb 4. PMID: 23385031.

57. Guerra-Mora JR, Perales-Caldera E, Aguilar-León D, Nava-Sanchez C, Díaz-Cruz A, Díaz-Martínez NE, Santillán-Doherty P, Torres-Villalobos G, Bravo-Reyna CC. Effects of Sildenafil and Tadalafil on Edema and Reactive Oxygen Species Production in an Experimental Model of Lung Ischemia-Reperfusion Injury. Transplant Proc. 2017 Jul-Aug;49(6):1461-1466. doi: 10.1016/j.transproceed.2017.03.089. PMID: 28736024.

58. Wietzikoski EGG, Foiatto JC, Czeczko NG, Malafaia O, Koleski FC, Mierzwa TC, Gomes RPX. Tadalafil protector effect during ischemia-reperfusion in rats. Acta Cir Bras. 2017 Nov;32(11):973-983. doi: 10.1590/s0102-865020170110000009. PMID: 29236802.

59. El-Sisi AE, Sokar SS, Abu-Risha SE, Ibrahim HA. Combination of tadalafil and diltiazem attenuates renal ischemia reperfusion-induced acute renal failure in rats. Biomed Pharmacother. 2016 Dec;84:861-869. doi: 10.1016/j.biopha.2016.10.009. Epub 2016 Oct 11. PMID: 27736652.

60. Ozdegirmenci O, Kucukozkan T, Akdag E, Topal T, Haberal A, Kayir H, Oter S, Akyol M, Uzbay T. Effects of sildenafil and tadalafil on ischemia/reperfusion injury in fetal rat brain. J Matern Fetal Neonatal Med. 2011 Feb;24(2):317-23. doi: 10.3109/14767058.2010.492061. Epub 2010 Jun 14. PMID: 20540678.

61. Soule BP, Hyodo F, Matsumoto K, Simone NL, Cook JA, Krishna MC, Mitchell JB. The chemistry and biology of nitroxide compounds. Free Radic Biol Med. 2007 Jun 1;42(11):1632-50. doi: 10.1016/j.freeradbiomed.2007.02.030. Epub 2007 Mar 12. PMID: 17462532; PMCID: PMC1991293.

62. Bi W, Bi L, Cai J, Liu S, Peng S, Fischer NO, Tok JB, Wang G. Dual-acting agents that possess free radical scavenging and antithrombotic activities: design, synthesis, and evaluation of phenolic tetrahydro-beta-carboline RGD peptide conjugates. Bioorg Med Chem Lett. 2006 Sep 1;16(17):4523-7. doi: 10.1016/j.bmcl.2006.06.024. Epub 2006 Jun 23. PMID: 16797986.

63. Kuznetsov AV, Javadov S, Sickinger S, Frotschnig S, Grimm M. H9c2 and HL-1 cells demonstrate distinct features of energy metabolism, mitochondrial function, and sensitivity to hypoxia-reoxygenation. *Biochim Biophys Acta*. 2015;1853(2):276-284. doi:10.1016/j.bbamcr.2014.11.015

64. Lindsey ML, Bolli R, Canty JM Jr, Du XJ, Frangogiannis NG, Frantz S, Gourdie RG, Holmes JW, Jones SP, Kloner RA, Lefer DJ, Liao R, Murphy E, Ping P, Przyklenk K, Recchia FA, Schwartz Longacre L, Ripplinger CM, Van Eyk JE, Heusch G. Guidelines for experimental models of myocardial ischemia and infarction. Am J Physiol Heart Circ Physiol. 2018 Apr 1;314(4):H812-H838. doi: 10.1152/ajpheart.00335.2017. Epub 2018 Jan 12. PMID: 29351451; PMCID: PMC5966768.

65. Chan DC. Mitochondrial Dynamics and Its Involvement in Disease. Annu Rev Pathol. 2020 Jan 24;15:235-259. doi: 10.1146/annurev-pathmechdis-012419-032711. Epub 2019 Oct 4. PMID: 31585519.

66. Li Q, Gao S, Kang Z, Zhang M, Zhao X, Zhai Y, Huang J, Yang GY, Sun W, Wang J. Rapamycin Enhances Mitophagy and Attenuates Apoptosis After Spinal Ischemia-Reperfusion Injury. Front Neurosci. 2018 Dec 3;12:865. doi: 10.3389/fnins.2018.00865. PMID: 30559639; PMCID: PMC6286985.

67. Yan J, Yan JY, Wang YX, Ling YN, Song XD, Wang SY, Liu HQ, Liu QC, Zhang Y, Yang PZ, Wang XB, Chen AH. Spermidine-enhanced autophagic flux improves cardiac dysfunction following myocardial infarction by targeting the AMPK/mTOR signalling pathway. Br J Pharmacol. 2019 Sep;176(17):3126-3142. doi: 10.1111/bph.14706. Epub 2019 Jul 17. PMID: 31077347; PMCID: PMC6692641.

68. Scherz-Shouval R, Elazar Z. Regulation of autophagy by ROS: physiology and pathology. Trends Biochem Sci. 2011 Jan;36(1):30-8. doi: 10.1016/j.tibs.2010.07.007. Epub 2010 Aug 20. PMID: 20728362.

69. Zhou J, Li XY, Liu YJ, Feng J, Wu Y, Shen HM, Lu GD. Full-coverage regulations of autophagy by ROS: from induction to maturation. Autophagy. 2022 Jun;18(6):1240-1255. doi: 10.1080/15548627.2021.1984656. Epub 2021 Oct 18. PMID: 34662529; PMCID: PMC9225210.

70. Takechi K, Tamura H, Yamaoka K, Sakurai H. Pharmacokinetic analysis of free radicals by in vivo BCM (Blood Circulation Monitoring)-ESR method. Free Radic Res. 1997 Jun;26(6):483-96. doi: 10.3109/10715769709097819. PMID: 9212342.

71. Klionsky DJ, Abdel-Aziz AK, Abdelfatah S, Abdellatif M, Abdoli A, Abel S, Abeliovich H, Abildgaard MH, Abudu YP, Acevedo-Arozena A, Adamopoulos IE, Adeli K, Adolph TE, Adornetto A, Aflaki E, Agam G, Agarwal A, Aggarwal BB, Agnello M, Agostinis P, Agrewala JN, Agrotis A, Aguilar PV, Ahmad ST, Ahmed ZM, Ahumada-Castro U, Aits S, Aizawa S, Akkoc Y, Akoumianaki T, Akpinar HA, Al-Abd AM, Al-Akra L, Al-Gharaibeh A, Alaoui-Jamali MA, Alberti S, Alcocer-Gómez E, Alessandri C, Ali M, Alim Al-Bari MA, Aliwaini S, Alizadeh J, Almacellas E, Almasan A, Alonso A, Alonso GD, Altan-Bonnet N, Altieri DC, Álvarez ÉMC, Alves S, Alves da Costa C, Alzaharna MM, Amadio M, Amantini C, Amaral C, Ambrosio S, Amer AO, Ammanathan V, An Z, Andersen SU, Andrabi SA, Andrade-Silva M, Andres AM, Angelini S, Ann D, Anozie UC, Ansari MY,

Antas P, Antebi A, Antón Z, Anwar T, Apetoh L, Apostolova N, Araki T, Araki Y, Arasaki K, Araújo WL, Araya J, Arden C, Arévalo MA, Arguelles S, Arias E, Arikkath J, Arimoto H, Ariosa AR, Armstrong-James D, Arnauné-Pelloquin L, Aroca A, Arroyo DS, Arsov I, Artero R, Asaro DML, Aschner M, Ashrafizadeh M, Ashur-Fabian O, Atanasov AG, Au AK, Auberger P, Auner HW, Aurelian L, Autelli R, Avagliano L, Ávalos Y, Aveic S, Aveleira CA, Avin-Wittenberg T, Aydin Y, Ayton S, Ayyadevara S, Azzopardi M, Baba M, Backer JM, Backues SK, Bae DH, Bae ON, Bae SH, Baehrecke EH, Baek A, Baek SH, Baek SH, Bagetta G, Bagniewska-Zadworna A, Bai H, Bai J, Bai X, Bai Y, Bairagi N, Baksi S, Balbi T, Baldari CT, Balduini W, Ballabio A, Ballester M, Balazadeh S, Balzan R, Bandopadhyay R, Banerjee S, Banerjee S, Bánréti Á, Bao Y, Baptista MS, Baracca A, Barbati C, Bargiela A, Barilà D, Barlow PG, Barmada SJ, Barreiro E, Barreto GE, Bartek J, Bartel B, Bartolome A, Barve GR, Basagoudanavar SH, Bassham DC, Bast RC Jr, Basu A, Batoko H, Batten I, Baulieu EE, Baumgarner BL, Bayry J, Beale R, Beau I, Beaumatin F, Bechara LRG, Beck GR Jr, Beers MF, Begun J, Behrends C, Behrens GMN, Bei R, Bejarano E, Bel S, Behl C, Belaid A, Belgareh-Touzé N, Bellarosa C, Belleudi F, Belló Pérez M, Bello-Morales R, Beltran JSO, Beltran S, Benbrook DM, Bendorius M, Benitez BA, Benito-Cuesta I, Bensalem J, Berchtold MW, Berezowska S, Bergamaschi D, Bergami M, Bergmann A, Berliocchi L, Berlioz-Torrent C, Bernard A, Berthoux L, Besirli CG, Besteiro S, Betin VM, Beyaert R, Bezbradica JS, Bhaskar K, Bhatia-Kissova I, Bhattacharya R, Bhattacharya S, Bhattacharyya S, Bhuiyan MS, Bhutia SK, Bi L, Bi X, Biden TJ, Bijian K, Billes VA, Binart N, Bincoletto C, Birgisdottir AB, Bjorkoy G, Blanco G, Blas-Garcia A, Blasiak J, Blomgran R, Blomgren K, Blum JS, Boada-Romero E, Boban M, Boesze-Battaglia K, Boeuf P, Boland B, Bomont P, Bonaldo P, Bonam SR, Bonfili L, Bonifacino JS, Boone BA, Bootman MD, Bordi M, Borner C, Bornhauser BC, Borthakur G, Bosch J, Bose S, Botana LM, Botas J, Boulanger CM, Boulton ME, Bourdenx M, Bourgeois B, Bourke NM, Bousquet G, Boya P, Bozhkov PV, Bozi LHM, Bozkurt TO, Brackney DE, Brandts CH, Braun RJ, Braus GH, Bravo-Sagua R, Bravo-San Pedro JM, Brest P, Bringer MA, Briones-Herrera A, Broaddus VC, Brodersen P, Brodsky JL, Brody SL, Bronson PG, Bronstein JM, Brown CN, Brown RE, Brum PC, Brumell JH, Brunetti-Pierri N, Bruno D, Bryson-Richardson RJ, Bucci C, Buchrieser C, Bueno M, Buitrago-Molina LE, Buraschi S, Buch S, Buchan JR, Buckingham EM, Budak H, Budini M, Bultynck G, Burada F, Burgoyne JR, Burón MI, Bustos V, Büttner S, Butturini E, Byrd A, Cabas I, Cabrera-Benitez S, Cadwell K, Cai J, Cai L, Cai Q, Cairó M, Calbet JA, Caldwell GA, Caldwell KA, Call JA, Calvani R, Calvo AC, Calvo-Rubio Barrera M, Camara NO, Camonis JH, Camougrand N, Campanella M, Campbell EM, Campbell-Valois FX, Campello S, Campesi I, Campos JC, Camuzard O, Cancino J, Candido de Almeida D, Canesi L, Caniggia I, Canonico B, Cantí C, Cao B, Caraglia M, Caramés B, Carchman EH, Cardenal-Muñoz E, Cardenas C, Cardenas L, Cardoso SM, Carew JS, Carle GF, Carleton G, Carloni S, Carmona-Gutierrez D, Carneiro LA, Carnevali O, Carosi JM, Carra S, Carrier A, Carrier L, Carroll B, Carter AB, Carvalho AN, Casanova M, Casas C, Casas J, Cassioli C, Castillo EF, Castillo K, Castillo-Lluva S, Castoldi F, Castori M, Castro AF, Castro-Caldas M, Castro-Hernandez J, Castro-Obregon S, Catz SD, Cavadas C, Cavaliere F, Cavallini G, Cavinato M, Cayuela ML, Cebollada Rica P, Cecarini V, Cecconi F, Cechowska-Pasko M, Cenci S, Ceperuelo-Mallafré V, Cerqueira JJ, Cerutti JM, Cervia D, Cetintas VB, Cetrullo S, Chae HJ, Chagin AS, Chai CY, Chakrabarti G, Chakrabarti O, Chakraborty T, Chakraborty T, Chami M, Chamilos G, Chan DW, Chan EYW, Chan ED, Chan HYE, Chan HH, Chan H, Chan MTV, Chan YS, Chandra PK, Chang CP, Chang C, Chang HC, Chang K, Chao J, Chapman T, Charlet-Berguerand N, Chatterjee S, Chaube SK, Chaudhary A, Chauhan S, Chaum E, Checler F, Cheetham ME, Chen CS, Chen GC, Chen JF, Chen LL, Chen L, Chen L, Chen M, Chen MK, Chen N, Chen Q, Chen RH, Chen S, Chen W, Chen W, Chen XM, Chen XW, Chen X, Chen Y, Chen YG, Chen Y, Chen Y, Chen YJ, Chen YQ, Chen ZS, Chen Z, Chen ZH, Chen ZJ, Chen Z, Cheng H, Cheng J, Cheng SY, Cheng W, Cheng X, Cheng XT, Cheng Y, Cheng Z, Chen Z, Cheong H, Cheong JK, Chernyak BV, Cherry S, Cheung CFR, Cheung CHA, Cheung KH, Chevet E, Chi RJ, Chiang AKS, Chiaradonna F, Chiarelli R, Chiariello M, Chica N, Chiocca S, Chiong M, Chiou SH, Chiramel AI, Chiurchiù V, Cho DH, Choe SK, Choi AMK, Choi ME, Choudhury KR, Chow NS, Chu CT, Chua JP, Chua JJE, Chung H, Chung KP, Chung S, Chung SH, Chung YL, Cianfanelli V, Ciechomska IA, Cifuentes M, Cinque L, Cirak S, Cirone M, Clague MJ, Clarke R, Clementi E, Coccia EM, Codogno P, Cohen E, Cohen MM, Colasanti T, Colasuonno F, Colbert RA, Colell A, Čolić M, Coll NS, Collins MO, Colombo MI, Colón-Ramos DA, Combaret L, Comincini S, Cominetti MR, Consiglio A, Conte A, Conti F, Contu VR, Cookson MR, Coombs KM, Coppens I, Corasaniti MT, Corkery DP, Cordes N, Cortese K, Costa MDC, Costantino S, Costelli P, Coto-Montes A, Crack PJ, Crespo JL,

Criollo A, Crippa V, Cristofani R, Csizmadia T, Cuadrado A, Cui B, Cui J, Cui Y, Cui Y, Culetto E, Cumino AC, Cybulsky AV, Czaja MJ, Czuczwar SJ, D'Adamo S, D'Amelio M, D'Arcangelo D, D'Lugos AC, D'Orazi G, da Silva JA, Dafsari HS, Dagda RK, Dagdas Y, Daglia M, Dai X, Dai Y, Dai Y, Dal Col J, Dalhaimer P, Dalla Valle L, Dallenga T, Dalmasso G, Damme M, Dando I, Dantuma NP, Darling AL, Das H, Dasarathy S, Dasari SK, Dash S, Daumke O, Dauphinee AN, Davies JS, Dávila VA, Davis RJ, Davis T, Dayalan Naidu S, De Amicis F, De Bosscher K, De Felice F, De Franceschi L, De Leonibus C, de Mattos Barbosa MG, De Meyer GRY, De Milito A, De Nunzio C, De Palma C, De Santi M, De Virgilio C, De Zio D, Debnath J, DeBosch BJ, Decuypere JP, Deehan MA, Deflorian G, DeGregori J, Dehay B, Del Rio G, Delaney JR, Delbridge LMD, Delorme-Axford E, Delpino MV, Demarchi F, Dembitz V, Demers ND, Deng H, Deng Z, Dengjel J, Dent P, Denton D, DePamphilis ML, Der CJ, Deretic V, Descoteaux A, Devis L, Devkota S, Devuyst O, Dewson G, Dharmasivam M, Dhiman R, di Bernardo D, Di Cristina M, Di Domenico F, Di Fazio P, Di Fonzo A, Di Guardo G, Di Guglielmo GM, Di Leo L, Di Malta C, Di Nardo A, Di Rienzo M, Di Sano F, Diallinas G, Diao J, Diaz-Araya G, Díaz-Laviada I, Dickinson JM, Diederich M, Dieudé M, Dikic I, Ding S, Ding WX, Dini L, Dinić J, Dinic M, Dinkova-Kostova AT, Dionne MS, Distler JHW, Diwan A, Dixon IMC, Djavaheri-Mergny M, Dobrinski I, Dobrovinskaya O, Dobrowolski R, Dobson RCJ, Đokić J, Dokmeci Emre S, Donadelli M, Dong B, Dong X, Dong Z, Dorn Ii GW, Dotsch V, Dou H, Dou J, Dowaidar M, Dridi S, Drucker L, Du A, Du C, Du G, Du HN, Du LL, du Toit A, Duan SB, Duan X, Duarte SP, Dubrovska A, Dunlop EA, Dupont N, Durán RV, Dwarakanath BS, Dyshlovoy SA, Ebrahimi-Fakhari D, Eckhart L, Edelstein CL, Efferth T, Eftekharpour E, Eichinger L, Eid N, Eisenberg T, Eissa NT, Eissa S, Ejarque M, El Andaloussi A, El-Hage N, El-Naggar S, Eleuteri AM, El-Shafey ES, Elgendy M, Eliopoulos AG, Elizalde MM, Elks PM, Elsasser HP, Elsherbiny ES, Emerling BM, Emre NCT, Eng CH, Engedal N, Engelbrecht AM, Engelsen AST, Enserink JM, Escalante R, Esclatine A, Escobar-Henriques M, Eskelinen EL, Espert L, Eusebio MO, Fabrias G, Fabrizi C, Facchiano A, Facchiano F, Fadeel B, Fader C, Faesen AC, Fairlie WD, Falcó A, Falkenburger BH, Fan D, Fan J, Fan Y, Fang EF, Fang Y, Fang Y, Fanto M, Farfel-Becker T, Faure M, Fazeli G, Fedele AO, Feldman AM, Feng D, Feng J, Feng L, Feng Y, Feng Y, Feng W, Fenz Araujo T, Ferguson TA, Fernández ÁF, Fernandez-Checa JC, Fernández-Veledo S, Fernie AR, Ferrante AW Jr, Ferraresi A, Ferrari MF, Ferreira JCB, Ferro-Novick S, Figueras A, Filadi R, Filigheddu N, Filippi-Chiela E, Filomeni G, Fimia GM, Fineschi V, Finetti F, Finkbeiner S, Fisher EA, Fisher PB, Flamigni F, Fliesler SJ, Flo TH, Florance I, Florey O, Florio T, Fodor E, Follo C, Fon EA, Forlino A, Fornai F, Fortini P, Fracassi A, Fraldi A, Franco B, Franco R, Franconi F, Frankel LB, Friedman SL, Fröhlich LF, Frühbeck G, Fuentes JM, Fujiki Y, Fujita N, Fujiwara Y, Fukuda M, Fulda S, Furic L, Furuya N, Fusco C, Gack MU, Gaffke L, Galadari S, Galasso A, Galindo MF, Gallolu Kankanamalage S, Galluzzi L, Galy V, Gammoh N, Gan B, Ganley IG, Gao F, Gao H, Gao M, Gao P, Gao SJ, Gao W, Gao X, Garcera A, Garcia MN, Garcia VE, García-Del Portillo F, Garcia-Escudero V, Garcia-Garcia A, Garcia-Macia M, García-Moreno D, Garcia-Ruiz C, García-Sanz P, Garg AD, Gargini R, Garofalo T, Garry RF, Gassen NC, Gatica D, Ge L, Ge W, Geiss-Friedlander R, Gelfi C, Genschik P, Gentle IE, Gerbino V, Gerhardt C, Germain K, Germain M, Gewirtz DA, Ghasemipour Afshar E, Ghavami S, Ghigo A, Ghosh M, Giamas G, Giampietri C, Giatromanolaki A, Gibson GE, Gibson SB, Ginet V, Giniger E, Giorgi C, Girao H, Girardin SE, Giridharan M, Giuliano S, Giulivi C, Giuriato S, Giustiniani J, Gluschko A, Goder V, Goginashvili A, Golab J, Goldstone DC, Golebiewska A, Gomes LR, Gomez R, Gómez-Sánchez R, Gomez-Puerto MC, Gomez-Sintes R, Gong Q, Goni FM, González-Gallego J, Gonzalez-Hernandez T, Gonzalez-Polo RA, Gonzalez-Reyes JA, González-Rodríguez P, Goping IS, Gorbatyuk MS, Gorbunov NV, Görgülü K, Gorojod RM, Gorski SM, Goruppi S, Gotor C, Gottlieb RA, Gozes I, Gozuacik D, Graef M, Gräler MH, Granatiero V, Grasso D, Gray JP, Green DR, Greenhough A, Gregory SL, Griffin EF, Grinstaff MW, Gros F, Grose C, Gross AS, Gruber F, Grumati P, Grune T, Gu X, Guan JL, Guardia CM, Guda K, Guerra F, Guerri C, Guha P, Guillén C, Gujar S, Gukovskaya A, Gukovsky I, Gunst J, Günther A, Guntur AR, Guo C, Guo C, Guo H, Guo LW, Guo M, Gupta P, Gupta SK, Gupta S, Gupta VB, Gupta V, Gustafsson AB, Gutterman DD, H B R, Haapasalo A, Haber JE, Hać A, Hadano S, Hafrén AJ, Haidar M, Hall BS, Halldén G, Hamacher-Brady A, Hamann A, Hamasaki M, Han W, Hansen M, Hanson PI, Hao Z, Harada M, Harhaji-Trajkovic L, Hariharan N, Haroon N, Harris J, Hasegawa T, Hasima Nagoor N, Haspel JA, Haucke V, Hawkins WD, Hay BA, Haynes CM, Hayrabedyan SB, Hays TS, He C, He Q, He RR, He YW, He YY, Heakal Y, Heberle AM, Hejtmancik JF, Helgason GV, Henkel V, Herb M, Hergovich A, Herman-Antosiewicz A, Hernández A, Hernandez C, Hernandez-Diaz S, Hernandez-Gea V, Herpin A,

Herreros J, Hervás JH, Hesselson D, Hetz C, Heussler VT, Higuchi Y, Hilfiker S, Hill JA, Hlavacek WS, Ho EA, Ho IHT, Ho PW, Ho SL, Ho WY, Hobbs GA, Hochstrasser M, Hoet PHM, Hofius D, Hofman P, Höhn A, Holmberg CI, Hombrebueno JR, Yi-Ren Hong CH, Hooper LV, Hoppe T, Horos R, Hoshida Y, Hsin IL, Hsu HY, Hu B, Hu D, Hu LF, Hu MC, Hu R, Hu W, Hu YC, Hu ZW, Hua F, Hua J, Hua Y, Huan C, Huang C, Huang C, Huang C, Huang C, Huang H, Huang K, Huang MLH, Huang R, Huang S, Huang T, Huang X, Huang YJ, Huber TB, Hubert V, Hubner CA, Hughes SM, Hughes WE, Humbert M, Hummer G, Hurley JH, Hussain S, Hussain S, Hussey PJ, Hutabarat M, Hwang HY, Hwang S, Ieni A, Ikeda F, Imagawa Y, Imai Y, Imbriano C, Imoto M, Inman DM, Inoki K, Iovanna J, Iozzo RV, Ippolito G, Irazoqui JE, Iribarren P, Ishaq M, Ishikawa M, Ishimwe N, Isidoro C, Ismail N, Issazadeh-Navikas S, Itakura E, Ito D, Ivankovic D, Ivanova S, Iyer AKV, Izquierdo JM, Izumi M, Jäättelä M, Jabir MS, Jackson WT, Jacobo-Herrera N, Jacomin AC, Jacquin E, Jadiya P, Jaeschke H, Jagannath C, Jakobi AJ, Jakobsson J, Janji B, Jansen-Dürr P, Jansson PJ, Jantsch J, Januszewski S, Jassey A, Jean S, Jeltsch-David H, Jendelova P, Jenny A, Jensen TE, Jessen N, Jewell JL, Ji J, Jia L, Jia R, Jiang L, Jiang Q, Jiang R, Jiang T, Jiang X, Jiang Y, Jimenez-Sanchez M, Jin EJ, Jin F, Jin H, Jin L, Jin L, Jin M, Jin S, Jo EK, Joffre C, Johansen T, Johnson GVW, Johnston SA, Jokitalo E, Jolly MK, Joosten LAB, Jordan J, Joseph B, Ju D, Ju JS, Ju J, Juárez E, Judith D, Juhász G, Jun Y, Jung CH, Jung SC, Jung YK, Jungbluth H, Jungverdorben J, Just S, Kaarniranta K, Kaasik A, Kabuta T, Kaganovich D, Kahana A, Kain R, Kajimura S, Kalamvoki M, Kalia M, Kalinowski DS, Kaludercic N, Kalvari I, Kaminska J, Kaminskyy VO, Kanamori H, Kanasaki K, Kang C, Kang R, Kang SS, Kaniyappan S, Kanki T, Kanneganti TD, Kanthasamy AG, Kanthasamy A, Kantorow M, Kapuy O, Karamouzis MV, Karim MR, Karmakar P, Katare RG, Kato M, Kaufmann SHE, Kauppinen A, Kaushal GP, Kaushik S, Kawasaki K, Kazan K, Ke PY, Keating DJ, Keber U, Kehrl JH, Keller KE, Keller CW, Kemper JK, Kenific CM, Kepp O, Kermorgant S, Kern A, Ketteler R, Keulers TG, Khalfin B, Khalil H, Khambu B, Khan SY, Khandelwal VKM, Khandia R, Kho W, Khobrekar NV, Khuansuwan S, Khundadze M, Killackey SA, Kim D, Kim DR, Kim DH, Kim DE, Kim EY, Kim EK, Kim HR, Kim HS, Hyung-Ryong Kim, Kim JH, Kim JK, Kim JH, Kim J, Kim JH, Kim KI, Kim PK, Kim SJ, Kimball SR, Kimchi A, Kimmelman AC, Kimura T, King MA, Kinghorn KJ, Kinsey CG, Kirkin V, Kirshenbaum LA, Kiselev SL, Kishi S, Kitamoto K, Kitaoka Y, Kitazato K, Kitsis RN, Kittler JT, Kjaerulff O, Klein PS, Klopstock T, Klucken J, Knævelsrud H, Knorr RL, Ko BCB, Ko F, Ko JL, Kobayashi H, Kobayashi S, Koch I, Koch JC, Koenig U, Kögel D, Koh YH, Koike M, Kohlwein SD, Kocaturk NM, Komatsu M, König J, Kono T, Kopp BT, Korcsmaros T, Korkmaz G, Korolchuk VI, Korsnes MS, Koskela A, Kota J, Kotake Y, Kotler ML, Kou Y, Koukourakis MI, Koustas E, Kovacs AL, Kovács T, Koya D, Kozako T, Kraft C, Krainc D, Krämer H, Krasnodembskaya AD, Kretz-Remy C, Kroemer G, Ktistakis NT, Kuchitsu K, Kuenen S, Kuerschner L, Kukar T, Kumar A, Kumar A, Kumar D, Kumar D, Kumar S, Kume S, Kumsta C, Kundu CN, Kundu M, Kunnumakkara AB, Kurgan L, Kutateladze TG, Kutlu O, Kwak S, Kwon HJ, Kwon TK, Kwon YT, Kyrmizi I, La Spada A, Labonté P, Ladoire S, Laface I, Lafont F, Lagace DC, Lahiri V, Lai Z, Laird AS, Lakkaraju A, Lamark T, Lan SH, Landajuela A, Lane DJR, Lane JD, Lang CH, Lange C, Langel Ü, Langer R, Lapaquette P, Laporte J, LaRusso NF, Lastres-Becker I, Lau WCY, Laurie GW, Lavandero S, Law BYK, Law HK, Layfield R, Le W, Le Stunff H, Leary AY, Lebrun JJ, Leck LYW, Leduc-Gaudet JP, Lee C, Lee CP, Lee DH, Lee EB, Lee EF, Lee GM, Lee HJ, Lee HK, Lee JM, Lee JS, Lee JA, Lee JY, Lee JH, Lee M, Lee MG, Lee MJ, Lee MS, Lee SY, Lee SJ, Lee SY, Lee SB, Lee WH, Lee YR, Lee YH, Lee Y, Lefebvre C, Legouis R, Lei YL, Lei Y, Leikin S, Leitinger G, Lemus L, Leng S, Lenoir O, Lenz G, Lenz HJ, Lenzi P, León Y, Leopoldino AM, Leschczyk C, Leskelä S, Letellier E, Leung CT, Leung PS, Leventhal JS, Levine B, Lewis PA, Ley K, Li B, Li DQ, Li J, Li J, Li J, Li K, Li L, Li M, Li M, Li M, Li M, Li M, Li PL, Li MQ, Li Q, Li S, Li T, Li W, Li W, Li X, Li YP, Li Y, Li Z, Li Z, Li Z, Lian J, Liang C, Liang Q, Liang W, Liang Y, Liang Y, Liao G, Liao L, Liao M, Liao YF, Librizzi M, Lie PPY, Lilly MA, Lim HJ, Lima TRR, Limana F, Lin C, Lin CW, Lin DS, Lin FC, Lin JD, Lin KM, Lin KH, Lin LT, Lin PH, Lin Q, Lin S, Lin SJ, Lin W, Lin X, Lin YX, Lin YS, Linden R, Lindner P, Ling SC, Lingor P, Linnemann AK, Liou YC, Lipinski MM, Lipovšek S, Lira VA, Lisiak N, Liton PB, Liu C, Liu CH, Liu CF, Liu CH, Liu F, Liu H, Liu HS, Liu HF, Liu H, Liu J, Liu J, Liu J, Liu L, Liu L, Liu M, Liu Q, Liu W, Liu W, Liu XH, Liu X, Liu X, Liu X, Liu Y, Liu Y, Liu Y, Liu Y, Liu Y, Livingston JA, Lizard G, Lizcano JM, Ljubojevic-Holzer S, LLeonart ME, Llobet-Navàs D, Llorente A, Lo CH, Lobato-Márquez D, Long Q, Long YC, Loos B, Loos JA, López MG, López-Doménech G, López-Guerrero JA, López-Jiménez AT, López-Pérez Ó, López-Valero I, Lorenowicz MJ, Lorente M, Lorincz P, Lossi L, Lotersztajn S, Lovat PE, Lovell JF, Lovy A, Lőw P, Lu G, Lu H, Lu JH, Lu JJ, Lu

 doi:10.20944/preprints202208.0352.v1

M, Lu S, Luciani A, Lucocq JM, Ludovico P, Luftig MA, Luhr M, Luis-Ravelo D, Lum JJ, Luna-Dulcey L, Lund AH, Lund VK, Lünemann JD, Lüningschrör P, Luo H, Luo R, Luo S, Luo Z, Luparello C, Lüscher B, Luu L, Lyakhovich A, Lyamzaev KG, Lystad AH, Lytvynchuk L, Ma AC, Ma C, Ma M, Ma NF, Ma QH, Ma X, Ma Y, Ma Z, MacDougald OA, Macian F, MacIntosh GC, MacKeigan JP, Macleod KF, Maday S, Madeo F, Madesh M, Madl T, Madrigal-Matute J, Maeda A, Maejima Y, Magarinos M, Mahavadi P, Maiani E, Maiese K, Maiti P, Maiuri MC, Majello B, Major MB, Makareeva E, Malik F, Mallilankaraman K, Malorni W, Maloyan A, Mammadova N, Man GCW, Manai F, Mancias JD, Mandelkow EM, Mandell MA, Manfredi AA, Manjili MH, Manjithaya R, Manque P, Manshian BB, Manzano R, Manzoni C, Mao K, Marchese C, Marchetti S, Marconi AM, Marcucci F, Mardente S, Mareninova OA, Margeta M, Mari M, Marinelli S, Marinelli O, Mariño G, Mariotto S, Marshall RS, Marten MR, Martens S, Martin APJ, Martin KR, Martin S, Martin S, Martín-Segura A, Martín-Acebes MA, Martin-Burriel I, Martin-Rincon M, Martin-Sanz P, Martina JA, Martinet W, Martinez A, Martinez A, Martinez J, Martinez Velazquez M, Martinez-Lopez N, Martinez-Vicente M, Martins DO, Martins JO, Martins WK, Martins-Marques T, Marzetti E, Masaldan S, Masclaux-Daubresse C, Mashek DG, Massa V, Massieu L, Masson GR, Masuelli L, Masyuk AI, Masyuk TV, Matarrese P, Matheu A, Matoba S, Matsuzaki S, Mattar P, Matte A, Mattoscio D, Mauriz JL, Mauthe M, Mauvezin C, Maverakis E, Maycotte P, Mayer J, Mazzoccoli G, Mazzoni C, Mazzulli JR, McCarty N, McDonald C, McGill MR, McKenna SL, McLaughlin B, McLoughlin F, McNiven MA, McWilliams TG, Mechta-Grigoriou F, Medeiros TC, Medina DL, Megeney LA, Megyeri K, Mehrpour M, Mehta JL, Meijer AJ, Meijer AH, Mejlvang J, Meléndez A, Melk A, Memisoglu G, Mendes AF, Meng D, Meng F, Meng T, Menna-Barreto R, Menon MB, Mercer C, Mercier AE, Mergny JL, Merighi A, Merkley SD, Merla G, Meske V, Mestre AC, Metur SP, Meyer C, Meyer H, Mi W, Mialet-Perez J, Miao J, Micale L, Miki Y, Milan E, Milczarek M, Miller DL, Miller SI, Miller S, Millward SW, Milosevic I, Minina EA, Mirzaei H, Mirzaei HR, Mirzaei M, Mishra A, Mishra N, Mishra PK, Misirkic Marjanovic M, Misasi R, Misra A, Misso G, Mitchell C, Mitou G, Miura T, Miyamoto S, Miyazaki M, Miyazaki M, Miyazaki T, Miyazawa K, Mizushima N, Mogensen TH, Mograbi B, Mohammadinejad R, Mohamud Y, Mohanty A, Mohapatra S, Möhlmann T, Mohmmed A, Moles A, Moley KH, Molinari M, Mollace V, Møller AB, Mollereau B, Mollinedo F, Montagna C, Monteiro MJ, Montella A, Montes LR, Montico B, Mony VK, Monzio Compagnoni G, Moore MN, Moosavi MA, Mora AL, Mora M, Morales-Alamo D, Moratalla R, Moreira PI, Morelli E, Moreno S, Moreno-Blas D, Moresi V, Morga B, Morgan AH, Morin F, Morishita H, Moritz OL, Moriyama M, Moriyasu Y, Morleo M, Morselli E, Moruno-Manchon JF, Moscat J, Mostowy S, Motori E, Moura AF, Moustaid-Moussa N, Mrakovcic M, Muciño-Hernández G, Mukherjee A, Mukhopadhyay S, Mulcahy Levy JM, Mulero V, Muller S, Münch C, Munjal A, Munoz-Canoves P, Muñoz-Galdeano T, Münz C, Murakawa T, Muratori C, Murphy BM, Murphy JP, Murthy A, Myöhänen TT, Mysorekar IU, Mytych J, Nabavi SM, Nabissi M, Nagy P, Nah J, Nahimana A, Nakagawa I, Nakamura K, Nakatogawa H, Nandi SS, Nanjundan M, Nanni M, Napolitano G, Nardacci R, Narita M, Nassif M, Nathan I, Natsumeda M, Naude RJ, Naumann C, Naveiras O, Navid F, Nawrocki ST, Nazarko TY, Nazio F, Negoita F, Neill T, Neisch AL, Neri LM, Netea MG, Neubert P, Neufeld TP, Neumann D, Neutzner A, Newton PT, Ney PA, Nezis IP, Ng CCW, Ng TB, Nguyen HTT, Nguyen LT, Ni HM, Ní Cheallaigh C, Ni Z, Nicolao MC, Nicoli F, Nieto-Diaz M, Nilsson P, Ning S, Niranjan R, Nishimune H, Niso-Santano M, Nixon RA, Nobili A, Nobrega C, Noda T, Nogueira-Recalde U, Nolan TM, Nombela I, Novak I, Novoa B, Nozawa T, Nukina N, Nussbaum-Krammer C, Nylandsted J, O'Donovan TR, O'Leary SM, O'Rourke EJ, O'Sullivan MP, O'Sullivan TE, Oddo S, Oehme I, Ogawa M, Ogier-Denis E, Ogmundsdottir MH, Ogretmen B, Oh GT, Oh SH, Oh YJ, Ohama T, Ohashi Y, Ohmuraya M, Oikonomou V, Ojha R, Okamoto K, Okazawa H, Oku M, Oliván S, Oliveira JMA, Ollmann M, Olzmann JA, Omari S, Omary MB, Önal G, Ondrej M, Ong SB, Ong SG, Onnis A, Orellana JA, Orellana-Muñoz S, Ortega-Villaizan MDM, Ortiz-Gonzalez XR, Ortona E, Osiewacz HD, Osman AK, Osta R, Otegui MS, Otsu K, Ott C, Ottobrini L, Ou JJ, Outeiro TF, Oynebraten I, Ozturk M, Pagès G, Pahari S, Pajares M, Pajvani UB, Pal R, Paladino S, Pallet N, Palmieri M, Palmisano G, Palumbo C, Pampaloni F, Pan L, Pan Q, Pan W, Pan X, Panasyuk G, Pandey R, Pandey UB, Pandya V, Paneni F, Pang SY, Panzarini E, Papademetrio DL, Papaleo E, Papinski D, Papp D, Park EC, Park HT, Park JM, Park JI, Park JT, Park J, Park SC, Park SY, Parola AH, Parys JB, Pasquier A, Pasquier B, Passos JF, Pastore N, Patel HH, Patschan D, Pattingre S, Pedraza-Alva G, Pedraza-Chaverri J, Pedrozo Z, Pei G, Pei J, Peled-Zehavi H, Pellegrini JM, Pelletier J, Peñalva MA, Peng D, Peng Y, Penna F, Pennuto M, Pentimalli F, Pereira CM, Pereira GJS, Pereira LC,

 doi:10.20944/preprints202208.0352.v1

Pereira de Almeida L, Perera ND, Pérez-Lara Á, Perez-Oliva AB, Pérez-Pérez ME, Periyasamy P, Perl A, Perrotta C, Perrotta I, Pestell RG, Petersen M, Petrache I, Petrovski G, Pfirrmann T, Pfister AS, Philips JA, Pi H, Picca A, Pickrell AM, Picot S, Pierantoni GM, Pierdominici M, Pierre P, Pierrefite-Carle V, Pierzynowska K, Pietrocola F, Pietruczuk M, Pignata C, Pimentel-Muiños FX, Pinar M, Pinheiro RO, Pinkas-Kramarski R, Pinton P, Pircs K, Piya S, Pizzo P, Plantinga TS, Platta HW, Plaza-Zabala A, Plomann M, Plotnikov EY, Plun-Favreau H, Pluta R, Pocock R, Pöggeler S, Pohl C, Poirot M, Poletti A, Ponpuak M, Popelka H, Popova B, Porta H, Porte Alcon S, Portilla-Fernandez E, Post M, Potts MB, Poulton J, Powers T, Prahlad V, Prajsnar TK, Praticò D, Prencipe R, Priault M, Proikas-Cezanne T, Promponas VJ, Proud CG, Puertollano R, Puglielli L, Pulinilkunnil T, Puri D, Puri R, Puyal J, Qi X, Qi Y, Qian W, Qiang L, Qiu Y, Quadrilatero J, Quarleri J, Raben N, Rabinowich H, Ragona D, Ragusa MJ, Rahimi N, Rahmati M, Raia V, Raimundo N, Rajasekaran NS, Ramachandra Rao S, Rami A, Ramírez-Pardo I, Ramsden DB, Randow F, Rangarajan PN, Ranieri D, Rao H, Rao L, Rao R, Rathore S, Ratnayaka JA, Ratovitski EA, Ravanan P, Ravegnini G, Ray SK, Razani B, Rebecca V, Reggiori F, Régnier-Vigouroux A, Reichert AS, Reigada D, Reiling JH, Rein T, Reipert S, Rekha RS, Ren H, Ren J, Ren W, Renault T, Renga G, Reue K, Rewitz K, Ribeiro de Andrade Ramos B, Riazuddin SA, Ribeiro-Rodrigues TM, Ricci JE, Ricci R, Riccio V, Richardson DR, Rikihisa Y, Risbud MV, Risueño RM, Ritis K, Rizza S, Rizzuto R, Roberts HC, Roberts LD, Robinson KJ, Roccheri MC, Rocchi S, Rodney GG, Rodrigues T, Rodrigues Silva VR, Rodriguez A, Rodriguez-Barrueco R, Rodriguez-Henche N, Rodriguez-Rocha H, Roelofs J, Rogers RS, Rogov VV, Rojo AI, Rolka K, Romanello V, Romani L, Romano A, Romano PS, Romeo-Guitart D, Romero LC, Romero M, Roney JC, Rongo C, Roperto S, Rosenfeldt MT, Rosenstiel P, Rosenwald AG, Roth KA, Roth L, Roth S, Rouschop KMA, Roussel BD, Roux S, Rovere-Querini P, Roy A, Rozieres A, Ruano D, Rubinsztein DC, Rubtsova MP, Ruckdeschel K, Ruckenstuhl C, Rudolf E, Rudolf R, Ruggieri A, Ruparelia AA, Rusmini P, Russell RR, Russo GL, Russo M, Russo R, Ryabaya OO, Ryan KM, Ryu KY, Sabater-Arcis M, Sachdev U, Sacher M, Sachse C, Sadhu A, Sadoshima J, Safren N, Saftig P, Sagona AP, Sahay G, Sahebkar A, Sahin M, Sahin O, Sahni S, Saito N, Saito S, Saito T, Sakai R, Sakai Y, Sakamaki JI, Saksela K, Salazar G, Salazar-Degracia A, Salekdeh GH, Saluja AK, Sampaio-Marques B, Sanchez MC, Sanchez-Alcazar JA, Sanchez-Vera V, Sancho-Shimizu V, Sanderson JT, Sandri M, Santaguida S, Santambrogio L, Santana MM, Santoni G, Sanz A, Sanz P, Saran S, Sardiello M, Sargeant TJ, Sarin A, Sarkar C, Sarkar S, Sarrias MR, Sarkar S, Sarmah DT, Sarparanta J, Sathyanarayan A, Sathyanarayanan R, Scaglione KM, Scatozza F, Schaefer L, Schafer ZT, Schaible UE, Schapira AHV, Scharl M, Schatzl HM, Schein CH, Scheper W, Scheuring D, Schiaffino MV, Schiappacassi M, Schindl R, Schlattner U, Schmidt O, Schmitt R, Schmidt SD, Schmitz I, Schmukler E, Schneider A, Schneider BE, Schober R, Schoijet AC, Schott MB, Schramm M, Schröder B, Schuh K, Schüller C, Schulze RJ, Schürmanns L, Schwamborn JC, Schwarten M, Scialo F, Sciarretta S, Scott MJ, Scotto KW, Scovassi AI, Scrima A, Scrivo A, Sebastian D, Sebti S, Sedej S, Segatori L, Segev N, Seglen PO, Seiliez I, Seki E, Selleck SB, Sellke FW, Selsby JT, Sendtner M, Senturk S, Seranova E, Sergi C, Serra-Moreno R, Sesaki H, Settembre C, Setty SRG, Sgarbi G, Sha O, Shacka JJ, Shah JA, Shang D, Shao C, Shao F, Sharbati S, Sharkey LM, Sharma D, Sharma G, Sharma K, Sharma P, Sharma S, Shen HM, Shen H, Shen J, Shen M, Shen W, Shen Z, Sheng R, Sheng Z, Sheng ZH, Shi J, Shi X, Shi YH, Shiba-Fukushima K, Shieh JJ, Shimada Y, Shimizu S, Shimozawa M, Shintani T, Shoemaker CJ, Shojaei S, Shoji I, Shravage BV, Shridhar V, Shu CW, Shu HB, Shui K, Shukla AK, Shutt TE, Sica V, Siddiqui A, Sierra A, Sierra-Torre V, Signorelli S, Sil P, Silva BJA, Silva JD, Silva-Pavez E, Silvente-Poirot S, Simmonds RE, Simon AK, Simon HU, Simons M, Singh A, Singh LP, Singh R, Singh SV, Singh SK, Singh SB, Singh S, Singh SP, Sinha D, Sinha RA, Sinha S, Sirko A, Sirohi K, Sivridis EL, Skendros P, Skirycz A, Slaninová I, Smaili SS, Smertenko A, Smith MD, Soenen SJ, Sohn EJ, Sok SPM, Solaini G, Soldati T, Soleimanpour SA, Soler RM, Solovchenko A, Somarelli JA, Sonawane A, Song F, Song HK, Song JX, Song K, Song Z, Soria LR, Sorice M, Soukas AA, Soukup SF, Sousa D, Sousa N, Spagnuolo PA, Spector SA, Srinivas Bharath MM, St Clair D, Stagni V, Staiano L, Stalnecker CA, Stankov MV, Stathopulos PB, Stefan K, Stefan SM, Stefanis L, Steffan JS, Steinkasserer A, Stenmark H, Sterneckert J, Stevens C, Stoka V, Storch S, Stork B, Strappazzon F, Strohecker AM, Stupack DG, Su H, Su LY, Su L, Suarez-Fontes AM, Subauste CS, Subbian S, Subirada PV, Sudhandiran G, Sue CM, Sui X, Summers C, Sun G, Sun J, Sun K, Sun MX, Sun Q, Sun Y, Sun Z, Sunahara KKS, Sundberg E, Susztak K, Sutovsky P, Suzuki H, Sweeney G, Symons JD, Sze SCW, Szewczyk NJ, Tabęcka-Łonczynska A, Tabolacci C, Tacke F, Taegtmeyer H, Tafani M, Tagaya M, Tai H, Tait SWG, Takahashi Y, Takats S, Talwar P, Tam C, Tam SY, Tampellini D, Tamura

 doi:10.20944/preprints202208.0352.v1

A, Tan CT, Tan EK, Tan YQ, Tanaka M, Tanaka M, Tang D, Tang J, Tang TS, Tanida I, Tao Z, Taouis M, Tatenhorst L, Tavernarakis N, Taylor A, Taylor GA, Taylor JM, Tchetina E, Tee AR, Tegeder I, Teis D, Teixeira N, Teixeira-Clerc F, Tekirdag KA, Tencomnao T, Tenreiro S, Tepikin AV, Testillano PS, Tettamanti G, Tharaux PL, Thedieck K, Thekkinghat AA, Thellung S, Thinwa JW, Thirumalaikumar VP, Thomas SM, Thomes PG, Thorburn A, Thukral L, Thum T, Thumm M, Tian L, Tichy A, Till A, Timmerman V, Titorenko VI, Todi SV, Todorova K, Toivonen JM, Tomaipitinca L, Tomar D, Tomas-Zapico C, Tomić S, Tong BC, Tong C, Tong X, Tooze SA, Torgersen ML, Torii S, Torres-López L, Torriglia A, Towers CG, Towns R, Toyokuni S, Trajkovic V, Tramontano D, Tran QG, Travassos LH, Trelford CB, Tremel S, Trougakos IP, Tsao BP, Tschan MP, Tse HF, Tse TF, Tsugawa H, Tsvetkov AS, Tumbarello DA, Tumtas Y, Tuñón MJ, Turcotte S, Turk B, Turk V, Turner BJ, Tuxworth RI, Tyler JK, Tyutereva EV, Uchiyama Y, Ugun-Klusek A, Uhlig HH, Ułamek-Kozioł M, Ulasov IV, Umekawa M, Ungermann C, Unno R, Urbe S, Uribe-Carretero E, Üstün S, Uversky VN, Vaccari T, Vaccaro MI, Vahsen BF, Vakifahmetoglu-Norberg H, Valdor R, Valente MJ, Valko A, Vallee RB, Valverde AM, Van den Berghe G, van der Veen S, Van Kaer L, van Loosdregt J, van Wijk SJL, Vandenberghe W, Vanhorebeek I, Vannier-Santos MA, Vannini N, Vanrell MC, Vantaggiato C, Varano G, Varela-Nieto I, Varga M, Vasconcelos MH, Vats S, Vavvas DG, Vega-Naredo I, Vega-Rubin-de-Celis S, Velasco G, Velázquez AP, Vellai T, Vellenga E, Velotti F, Verdier M, Verginis P, Vergne I, Verkade P, Verma M, Verstreken P, Vervliet T, Vervoorts J, Vessoni AT, Victor VM, Vidal M, Vidoni C, Vieira OV, Vierstra RD, Viganó S, Vihinen H, Vijayan V, Vila M, Vilar M, Villalba JM, Villalobo A, Villarejo-Zori B, Villarroya F, Villarroya J, Vincent O, Vindis C, Viret C, Viscomi MT, Visnjic D, Vitale I, Vocadlo DJ, Voitsekhovskaja OV, Volonté C, Volta M, Vomero M, Von Haefen C, Vooijs MA, Voos W, Vucicevic L, Wade-Martins R, Waguri S, Waite KA, Wakatsuki S, Walker DW, Walker MJ, Walker SA, Walter J, Wandosell FG, Wang B, Wang CY, Wang C, Wang C, Wang C, Wang CY, Wang D, Wang F, Wang F, Wang F, Wang G, Wang H, Wang H, Wang H, Wang HG, Wang J, Wang J, Wang J, Wang J, Wang K, Wang L, Wang L, Wang MH, Wang M, Wang N, Wang P, Wang P, Wang P, Wang P, Wang QJ, Wang Q, Wang QK, Wang QA, Wang WT, Wang W, Wang X, Wang X, Wang Y, Wang Y, Wang Y, Wang YY, Wang Y, Wang Y, Wang Y, Wang Y, Wang Z, Wang Z, Wang Z, Warnes G, Warnsmann V, Watada H, Watanabe E, Watchon M, Wawrzyńska A, Weaver TE, Wegrzyn G, Wehman AM, Wei H, Wei L, Wei T, Wei Y, Weiergräber OH, Weihl CC, Weindl G, Weiskirchen R, Wells A, Wen RH, Wen X, Werner A, Weykopf B, Wheatley SP, Whitton JL, Whitworth AJ, Wiktorska K, Wildenberg ME, Wileman T, Wilkinson S, Willbold D, Williams B, Williams RSB, Williams RL, Williamson PR, Wilson RA, Winner B, Winsor NJ, Witkin SS, Wodrich H, Woehlbier U, Wollert T, Wong E, Wong JH, Wong RW, Wong VKW, Wong WW, Wu AG, Wu C, Wu J, Wu J, Wu KK, Wu M, Wu SY, Wu S, Wu SY, Wu S, Wu WKK, Wu X, Wu X, Wu YW, Wu Y, Xavier RJ, Xia H, Xia L, Xia Z, Xiang G, Xiang J, Xiang M, Xiang W, Xiao B, Xiao G, Xiao H, Xiao HT, Xiao J, Xiao L, Xiao S, Xiao Y, Xie B, Xie CM, Xie M, Xie Y, Xie Z, Xie Z, Xilouri M, Xu C, Xu E, Xu H, Xu J, Xu J, Xu L, Xu WW, Xu X, Xue Y, Yakhine-Diop SMS, Yamaguchi M, Yamaguchi O, Yamamoto A, Yamashina S, Yan S, Yan SJ, Yan Z, Yanagi Y, Yang C, Yang DS, Yang H, Yang HT, Yang H, Yang JM, Yang J, Yang J, Yang L, Yang L, Yang M, Yang PM, Yang Q, Yang S, Yang S, Yang SF, Yang W, Yang WY, Yang X, Yang X, Yang Y, Yang Y, Yao H, Yao S, Yao X, Yao YG, Yao YM, Yasui T, Yazdankhah M, Yen PM, Yi C, Yin XM, Yin Y, Yin Z, Yin Z, Ying M, Ying Z, Yip CK, Yiu SPT, Yoo YH, Yoshida K, Yoshii SR, Yoshimori T, Yousefi B, Yu B, Yu H, Yu J, Yu J, Yu L, Yu ML, Yu SW, Yu VC, Yu WH, Yu Z, Yu Z, Yuan J, Yuan LQ, Yuan S, Yuan SF, Yuan Y, Yuan Z, Yue J, Yue Z, Yun J, Yung RL, Zacks DN, Zaffagnini G, Zambelli VO, Zanella I, Zang QS, Zanivan S, Zappavigna S, Zaragoza P, Zarbalis KS, Zarebkohan A, Zarrouk A, Zeitlin SO, Zeng J, Zeng JD, Žerovnik E, Zhan L, Zhang B, Zhang DD, Zhang H, Zhang H, Zhang H, Zhang H, Zhang H, Zhang H, Zhang H, Zhang HL, Zhang J, Zhang J, Zhang JP, Zhang KYB, Zhang LW, Zhang L, Zhang L, Zhang L, Zhang L, Zhang M, Zhang P, Zhang S, Zhang W, Zhang X, Zhang XW, Zhang X, Zhang X, Zhang X, Zhang X, Zhang XD, Zhang Y, Zhang Y, Zhang Y, Zhang YD, Zhang Y, Zhang YY, Zhang Y, Zhang Z, Zhang Z, Zhang Z, Zhang Z, Zhang Z, Zhang Z, Zhao H, Zhao L, Zhao S, Zhao T, Zhao XF, Zhao Y, Zhao Y, Zhao Y, Zhao Y, Zheng G, Zheng K, Zheng L, Zheng S, Zheng XL, Zheng Y, Zheng ZG, Zhivotovsky B, Zhong Q, Zhou A, Zhou B, Zhou C, Zhou G, Zhou H, Zhou H, Zhou H, Zhou J, Zhou J, Zhou J, Zhou J, Zhou K, Zhou R, Zhou XJ, Zhou Y, Zhou Y, Zhou Y, Zhou ZY, Zhou Z, Zhu B, Zhu C, Zhu GQ, Zhu H, Zhu H, Zhu H, Zhu WG, Zhu Y, Zhu Y, Zhuang H, Zhuang X, Zientara-Rytter K, Zimmermann CM, Ziviani E, Zoladek T, Zong WX, Zorov DB, Zorzano A, Zou W, Zou Z, Zou Z, Zuryn S, Zwerschke W, Brand-Saberi B, Dong XC,

Kenchappa CS, Li Z, Lin Y, Oshima S, Rong Y, Sluimer JC, Stallings CL, Tong CK. Guidelines for the use and interpretation of assays for monitoring autophagy (4th edition)[1]. Autophagy. 2021 Jan;17(1):1-382. doi: 10.1080/15548627.2020.1797280. Epub 2021 Feb 8. PMID: 33634751; PMCID: PMC7996087.